SOD/Catalase Mimetic Platinum Nanoparticles Protects from X-irradiation and Cold Atmospheric Plasma induced Apoptosis via Suppression of ROS

PARAS JAWAID

Department of Radiological Sciences

Graduate School of Medicine and Pharmaceutical Sciences

University of Toyama

2016

SOD/Catalase Mimetic Platinum Nanoparticles Protects from X-irradiation and Cold Atmospheric Plasma induced Apoptosis via Suppression of ROS

DISSERTATION

SUBMITTED TO THE FACULTY OF MEDICINE

UNIVERSITY OF TOYAMA

FOR THE FULLFILLMENT OF A DEGREE OF

DOCTOR OF PHILOSOPHY IN MEDICINE

PARAS JAWAID

Department of Radiological Sciences

Graduate School of Medicine and Pharmaceutical Sciences

University of Toyama

2016

TABLE OF CONTENTS

Abbreviations ……..…….… 6

Chapter 1

General Introduction

1.1 Nanomedicine …….……...……...……...…… 8

1.1.1 Platinum nanoparticles

1.2 X-irradiation ……..…….……...…..…….……..…9

1.3 Cold atmospheric plasma ……..……..……..…. 10

Chapter 2

2.1 Material and Methods ……..……..……. 12

2.2.1 Preparation of Pt-NPs

2.2.2 Cell culture

2.2.3 X-irradiation system

2.2.4 Cold atmospheric plasma system

2.2.5 Electron microscopy

2.2.6 DNA Fragmentation

2.2.7 Annexin V-FITC/ PI staining

2.2.8 Morphological detection of apoptosis

2.2.9 Cell Viability

2.2.10 Cell counting

2.2.11 Mitochondrial transmembrane potential (MMP)

2.2.12 Detection of intracellular free calcium ions

2.2.13 Assessment of intracellular ROS

2.2.14 Cell cycle analysis

2.2.15 Detection of Fas on cell surface

2.2.16 Measurement of caspase-8 activity

2.2.17 Western blotting
2.2.18 Statistical analysis

Chapter 3

Effects of platinum nanoparticles on radiation-induced apoptosis in human lymphoma U937 cells

3.1 Summary ……. 22
3.2 Specific research work ……... 23
3.2.1 Effects of Pt-NPs on x-irradiation-induced apoptosis
3.2.2 Suppression of intracellular ROS by Pt-NPs
3.2.3 Suppression of Fas receptor externalization by Pt-NPs
3.2.4 Assessment of intracellular caspase 8 activities
3.2.5 Effects of Pt-NPs on the mitochondrial pathway
3.2.6 Effects of Pt-NPs on expression of apoptotic related proteins
3.3 Discussion……..... 26
3.4 Conclusion …….... 29
3.5 Figures and Illustration …… 30

Chapter 4

Platinum nanoparticles prevent from Helium based cold atmospheric plasma-induced apoptosis

4.1 Summary ……. 44
4.2 Specific research work ……... 45
4.2.1 Effects of He-CAP on cell viability and apoptosis
4.2.2 Effects of Pt-NPs on He-CAP-induced apoptosis
4.2.3 Effects of Pt-NPs on He-CAP-induced cell cycle distribution
4.2.4 Effect of Pt-NPs on He-CAP-induced reactive oxygen species (ROS) generation

4.2.5 Measurement of mitochondrial membrane damage
4.2.6 Effect of Pt-NPs on intracellular $[Ca^{2+}]_i$ levels
4.2.7 Expression of apoptosis-related proteins
4.2.8 Effect of Pt-NPs on He-CAP-induced FAS externalization and caspase-8 activation
4.2.9 Effects of Pt-NPs on He-CAP-induced apoptosis in other cancer cell lines

4.3 Discussion……..... 50
4.4 Conclusion……..... 53
4.5 Figures, Table and Illustration……55

References ……..…..…. 71
Publications …….…….... 80
Acknowledgements …….. 81

Abbreviations

X-rays	X-irradiation
SOD	Superoxide dismutase
Pt-NPs	Platinum nanoparticles
He	Helium
CAP	Cold atmospheric plasma
ROS	Reactive oxygen species
(O_2^{-})	Superoxide
H_2O_2	Hydrogen peroxide
$^{\cdot}OH$	Hydroxyl radical
MMP	Mitochondrial membrane potential
OCl^{-}	Hypochlorite
$NO^{\cdot}$	Nitric oxide
$ONOO^{\cdot-}$	Peroxynitrite

Chapter 1

General introduction

1.1 Nanomedicine

Recently, nanotechnology is becoming popular due to the wide application of nanoparticles not only in material science but also in medical science [1]. Nano-technology, deals with the features as small as 1 billion of a meter. The broad application of nanotechnology covered almost all fields of life including nanomaterials, nanoscale devices, instrumentation research and biomedical research. The application of nanotechnology in the field of medicine is defined as nanomedicine, which deals with the biology, chemistry, engineering and medicine. It provides help in the use of nanoscale materials and devices for diagnosis and drug delivery, without occluding needles and capillaries, improve disease prevention, diagnosis and treatment of disorders such as cancer [1- 3].

1.1.1 Platinum nanoparticles

The medicinal use of platinum (Pt)-based compounds has gained attention since the discovery of the antitumor activity of *cis*-Diamminedichloroplatinum (cis-platin; discovered in 1960 and approved for clinical use in 1978) [2]. Platinum nanoparticles (Pt-NPs) are known to function as reductive catalysts; and have attracted attention in recent years due to the fact that, they may be used as an antioxidants to scavenge ROS persistently and catalytically in living organisms [1]. In fact, Pt-NPs possess the ability to scavenge superoxide and peroxide, showing that they act as superoxide dismutase (SOD)/catalase mimetics [3]. Pt-NPs have also been shown to induce DNA damage and p53-mediated growth arrest [4].

Platinum-based therapeutic drugs, notably cisplatin and carboplatin, have been

exploited in chemotherapy to kill cancer cells [2]. On the other hand, NPs of some noble metals, including platinum, function as reducing catalysts due to the large surface area [1]. The large surface area of small particles can potentiate the catalytic activity of metals, whose colloidal forms contribute to efficient catalysis with high electron holding at the surface [1,5,6]. In biological systems, this ability has been regarded as superoxide dismutase (SOD)/catalase mimetic activity, which could be useful for the prevention of a number of oxidative-stress associated pathologies [7,8]. Therefore, it is quite evident that Pt-NPs in a biological system can exert differential effects including cancer prevention and treatment.

Previously it was reported that Pt-NPs effectively protects against UV-induced inflammation and apoptosis by decreasing ROS production [7]. In our previous study we have found that the treatment of Pt-NPs in combination with hyperthermia was able to reverse the HT-induced apoptosis through a suppression of all the involved micro-molecular pathways [3]. The Pt-NPs used in this study were capped with polyacrylate (PAA), which make them stable in their colloidal solution [6]. These PAA-capped Pt-NPs have been reported to be superior to EUK-8, a well known SOD/catalase mimetic [9]; in addition their in *vivo* activity has also been well established [8].

1.2 X-irradiation

X-irradiation (X-rays) is well known to induce apoptosis over a certain dose. Two types of actions occur in the result to contribute for typical biological effects of ionizing radiation that are direct and indirect action. Cell damage due to the direct

ionization of macromolecules due to interaction between photons and DNA molecules refer to direct action of X-rays whereas in indirect action; radiolysis of water molecules, such as ·OH radicals react with DNA in the cells [10, 11]. It has been known that most of X-rays induced cell death is due to indirect action. On the other hand, mitochondria-dependent generation of reactive oxygen species (ROS) plays a central role in X-rays induced apoptosis, G2/M arrest, release of caspase activators and regulation of Bcl-2 family proteins [12, 13]. One of the most important ROS is hydroxyl radical; if this ROS will not be scavenged then it plays a cardinal role in the cell damage by inducing oxidative injuries of DNA and protein and lipid peroxidation of membranes [14-16, 11]. To overcome the harmful effects of X-rays catalase mimetics have been suggested to be co-administered in order to reduce the ROS mediated damage to normal tissues.

1.3 Cold atmospheric Plasma

Plasma medicine is a rapidly growing interdisciplinary field combining engineering, physics, biochemistry and life sciences [17]. Plasma, which has been regarded as the “fourth state of matter,” is a partially neutral ionized gas, which contains a mixture of electrons, photons, atoms, positive and negative ions, radicals, and various excited and non-excited molecules [18]. Plasma is classified into two categories on the basis of the temperature application, namely “thermal” and “non-thermal” or “cold” atmospheric plasma. In general, non-thermal or cold atmospheric plasma (CAP) is produced by applying a high voltage electric field at low pressures and power. Theoretically, it has been mentioned that any gas can be used to generate CAP [19].

However, intensive research has been focused on the use of helium and argon because these noble gases are monatomic and chemically inert, which results in the production of a stable plasma [20]. The use of helium has advantages over that of argon, it induces ionization at lower voltages and generates more ROS [21].

CAP has been found to be highly effective for biological and medical purposes including cancer treatment [22-27]. Several studies have shown the efficacy of CAP for cancer treatment and suggest that non-thermal plasma can induce apoptosis of cancer cells in a dose-dependent manner [27]. However, the exact molecular-mechanisms and signaling pathways are still not clear. CAP plasma can generate ROS mainly superoxide, peroxide, oxygen, and hydroxyl radicals. Therefore, mounting evidence suggests that the effects of CAP plasma are mainly mediated via generation of ROS [28] and lead to apoptosis [27], cellular necrosis [29], and senescence [30]. Although, cancer cells are particularly sensitive to ROS, in real clinical situations, it is very difficult to treat cancer with a single modality. Rather, multi-modality therapeutic strategy is adopted, one such possible application is the use of nanoparticles in combination with He-CAP. To date, there has been no report on the effects of nanoparticles on He-CAP-induced ROS generation and apoptosis.

Chapter 2

Material and Methods

2.1 Preparation of Pt-NPs

Pt-NPs were prepared by the citrate reduction of H_2PtC_{l6}, according to a previous report with minor modifications [1]. The original molarity of platinum was 1 mM. To make require concentration diluted with RPMI 1640 medium containing 10% fetal bovine serum to a final concentration of 100, 200, 300 and 500 μM.

2.2 Cell culture

Human myelomonocytic lymphoma U937, Hela, HCT-116, Molt-4 and Jurkat-T cell lines were obtained from Human Sciences Research Resource Bank (Japan Human Sciences Foundation, Tokyo, Japan). The U937, Molt-4 and Jurkat-T cells were grown in RPMI 1640 culture medium, Hela and HCT-116 cells were grown in DMEM supplemented with 10 % heat-inactivated fetal bovine serum (FBS) at 37 °C in humidified air with 5 % CO_2.

2.3 X-irradiation system

A 6-cm diameter plastic culture dish that containing 2 ml of the sample was prepared for X-rays with or without pre-treatment with Pt-NPs for 24 h at 37 °C. X-rays was carried out at room temperature by X-rays apparatus (MBR-1520R- 3, Hitachi Medico Technology Co., Kashiwa, Japan) operating at 150 kV and 20 mA, at a dose rate of 5 Gy/min as determined by Fricke dosimetry. After treatment, the cells were incubated at 37 °C with 5 % CO^2 and then harvested after 6 h for apoptosis evaluation.

2.4 Cold atmospheric helium plasma irradiation system

A cold atmospheric plasma system (PN-120TPG, NU Global, Japan) consisted of a gas flow controller, a voltage power supply and a hand-piece of the plasma jet, constructing an inner micro-hollow-type electrode and an outer dielectric barrier

electrode. The inner and outer diameter of dielectric tube was 1 and 2 mm, respectively. A high voltage power with a frequency of 60 Hz and a peak-to-peak voltage of 7 kV was supplied to the two electrodes. Helium gas with a gas flow rate of 2L/min was applied in this study for the generation of a plasma jet. The line-averaged electron density in the plasma source is approximately 2 x 10^{15} cm^{-3}. The length of the plasma jet was approximately 20 mm in atmospheric ambient. The gas temperature of the plasma jet was below 350 K.

2.5 Electron microscopy

The sample was collected and fixed with Karnovsky fixative in 0.1 M cacodylate buffer for two hours and 1 % osmium tetroxide for one hour at 41°C. The tissues were dehydrated through a graded ethanol series and embedded in Epon 812. Ultrathin sections were cut using an ultramicrotome (Reichert Ultracut S, Reichert, Vienna, Austria), stained with saturated uranyl acetate and lead citrate and observed under a transmission electron microscope (Hitachi H-7100, Hitachi Co. Ltd., Tokyo, Japan). The disruptions area of the basal lamina were counted under the electron microscope at a magnification of ×12,000 and expressed as the mean number in ten random fields.

2.6 DNA Fragmentation assay

For the detection of apoptosis the percentage of DNA fragmentation was assessed 6 h post treatment using the method of Sellins and Cohen [31] with minor modifications. Briefly, approximately 3 x 10^6 cells were lysed using 200 µl of lysis buffer (10 mM Tris, 1 mM EDTA and 0.2 % Triton X- 100, pH 7.5) and centrifuged at 13,000g for 10 min. Subsequently, each DNA sample in the supernatant and the

resulting pellet was precipitated in the 25 % trichloroacetic acid (TCA) at 4 °C overnight and quantified using a diphenylamine reagent after hydrolysis in 5 % TCA at 90 °C for 20 min. The percentage of fragmented DNA in each sample was calculated as the amount of DNA in the supernatant divided by total DNA for that sample (supernatant plus pellet).

2.7 Annexin V-FITC/ PI staining

To determine early apoptosis and secondary necrosis, phosphatidylserine (PS) externalization of apoptosis was determined by analysis of propidium iodide (PI) and fluorescein isothiocyanate (FITC)-labeled annexin V (Immunotech, Marseille, France) using Flow cytometry (Epics XL, Beckman-Coulter, Miami, FL) according to the instruction of the manufacturer. After the treatments, the remaining intact cells were incubated at 37 °C for 6 h, collected, washed with cold PBS at 4 °C and centrifuged at 1,200 rpm for 3 min. The resulting pellet was mixed with the binding buffer of the Annexin V-FITC kit. FITC labeled annexin V (5 µl) and PI (5 µl) were added to the 490 µl suspension and mixed gently. After incubation at 4 °C for 20 min in the dark, the cells were analyzed with a flow cytometry.

2.8 Morphological detection of apoptosis

The morphological changes in the cells were examined by Giemsa staining. After 6 and 24 h of incubation at 37 °C, the cells were harvested by centrifugation and washed by PBS. Then the cells were fixed with methanol and acetic acid (3:1) and spread on the glass slides. After drying, staining was performed with 5% Giemsa solution (pH 6.8) for 5 min.

2.9 Cell viability

The trypan blue exclusion test was performed by mixing 50 μl of a cell suspension with an equal amount of 0.3 % trypan blue solution (Sigma, St. Louis, MO) in PBS. After 3 min of incubation at room temperature, the numbers of stained cells and unstained cells were counted using a Burker Turk hemocytometer to estimate the number of intact non-viable cells and viable cells, respectively.

2.10 Cell counting

Cells were counted to determine the increase in cell count post-treatment. Samples of each treatment were collected and counted using a Burker Turk hemocytometer.

2.11 Mitochondrial transmembrane potential:

The cationic fluorophore, tetramethylrhodamine methyl ester (TMRM) (Molecular Probes, Eugene, OR), accumulated electrophoretically in mitochondria in response to MMP and was released upon loss of MMP. After the treatments, the cells were incubated at 37 °C for 6 h collected, washed with PBS and centrifuged at 1,200 rpm for 3 min. Then the cells were stained with the 10 nM TMRM for 15 min at 37 °C in 1 ml of PBS, followed by the immediate flow cytometry of red TMRM fluorescence (excitation at 488 nm; emission at 575 nm).

2.12 Detection of intracellular free calcium ions

Changes in intracellular free Ca^{2+} were determined after different treatments. $[Ca^{2+}]_i$ was measured using the calcium probe Fluo-3/AM (Dojindo Laboratories Co., Ltd., Kumamoto, Japan). The cells were harvested and then loaded with 5 μM Fluo-3/AM for 30 min at 37 °C. Excess Fluo-3/AM was removed by washing three times

with PBS. The fluorescence intensity of free Ca^{2+} level was measured by flow cytometry.

2.13 Assessment of intracellular ROS:

Evaluation of intracellular ROS in U937 cells was performed by flow cytometry using the fluorescence generate in the cells loaded with the sensitive fluorescent probes, a H_2O_2 sensitive dye, dichlorofluorescein diacetate (DCFH-DA) (Molecular probes, Eugene, OR). DCFH-DA rapidly diffuses in to the cytosol of cells where it is hydrolyzed to the non-fluorescent, oxidation sensitive DCFH. In the presence of cytosolic peroxide, DCFH is rapidly oxidized to the non-diffusible, fluorescent DCF [32]. Hydroethidine (HE) (Molecular Probes, Eugene, OR) was used to determine superoxide generation O_2^- by using the method of Gorman et al. HE is a reduced non-fluorescent precursor that, in the presence of superoxide anion species is readily oxidized intracellularly which intercalates into DNA and can be detected owing to its red fluorescence. 2-[6-(4′-hydroxy)phenoxy-3*H*-xanthen-3-on-9-yl] benzoic HPF and 2-[6-(4′-amino)phenoxy-3*H*-xanthen-3-on-9-yl] APF (Seikisui medical co., Tokyo, Japan) fluorescence probes are used to determine some species of ROS (OCl^-, ONOO, NO, $^{\cdot}OH$) in terms of an increase fluorescence and that are highly resistant to autoxidation [33]. The DCFH-DA was added at final concentration of 10 μM, HE, APF and HPF were added at final concentration of 5 μM and incubated for 15 min at 37 °C then cells were harvested 0, 3 and 6 h after post-treatment and the fraction of fluorescence positive cells was measured by flow cytometry as the proportion of cells containing intracellular ROS.

2.14 Cell cycle analysis

For flow cytometry, cells were fixed with 70 % ice cold ethanol, stored

overnight at −20 °C, and subsequently treated with 0.25 mg/ml RNase A (Nacalai Tesque, Kyoto, Japan) and 50 μg/ml PI to obtain the distribution of PI-based cell-cycle phases. The samples were finally run on an Epics XL flow cytometer (Beckman Coulter, Fullerton, CA).

2.15 Detection of Fas on cell surface

Cells (1 x 10^6) were washed twice with ice cold PBS, re-suspended in 20 μl of washing buffer containing 2.5 μg/ml of FITC conjugated anti-Fas monoclonal antibody (clone: UB3, MBL, Nagoya, Japan) and incubated for 30 min at room temperature. After staining cells were washed again with ice cold PBS and re-suspended in PBS. Data were analyzed by using the flow cytometry.

2.16 Measurement of caspase-8 activity

To measure caspase-8 activity, a FLICE/caspase-8 colorimetric protease assay kit (MBL, Nagoya, Japan) was used according to the manufacturer's instructions. The assay was based on the spectrophotometric detection of chromophore p-nitroanilide (pNA). The cells were harvested, lysed, and the protein lysate was collected. The protein samples (100 μg) were mixed with 50 μl of 10 mM dithiothreitol (DTT) at a final concentration of 200 μM. The mixtures were then incubated at 37 °C for 5 h and then the activity was measured at 400 nm using a spectrophotometer (Beckman Instruments Inc., Fullerton, CA).

2.17 Western blotting

Cells were collected and washed with cold PBS. They were lysed at a density of 2.5 x 10^6 cells／70 μl of RIPA buffer (50 mM Tris-HCl, 150 mM NaCl, 1 % Nonidet P-40 (v／v), 1 % sodium deoxycholate, 0.05 % SDS, 1 μg of each aprotinin, pepstatin

and leupeptin and 1mm phenylmethyl sulfonyl fluoride) for 20 min. Following brief sonification, the lysates were centrifuged at 12,000 g for 10 min at 4 °C, and the protein content in the supernatant was measured using the Bio- Rad protein assay kit (Bio-Rad, Hercules, CA). Protein lysates were denatured at 96 °C for 5 min after mixing with 2 μl SDS-loading buffers, applied on an SDS-polyacrylamide gel for electrophoresis, and transferred to nitrocellulose membrane. Western blot analysis was performed to detect caspase-3, XIAP, Bid, Bax, Bcl-2, Bcl-xl and Fas expressions using specific antibodies. Antibodies were obtained from Cell Signaling technology (Danvers, MA). Blots were then probed with either secondary horseradish peroxide (HRP)-conjugated anti-rabbit or anti-mouse IgG antibodies obtained from Cell Signaling. Band signals were visualized on a luminescent image analyzer (LAS 4000, Fujifilm Co., Tokyo, Japan) by using chemi-luminescence ECL detection reagents (Amersham Biosciences, Buckinghamshire, UK).

For the preparation of cytosolic extracts, 5 x 10^7cells were harvested and wash with 10 ml ice-cold PBS then centrifuge at 600 g for 5 min and remove supernatant. Re-suspend cells with 300 μl of 1x Cytosol Extraction Buffer Mix containing DTT and a Protease inhibitor according to the manufacturer`s instruction then incubate on ice for 10 min. Homogenize cells in an ice-cold dounce tissue grinder and then centrifuge at 3,000 rpm for 10 min at 4 °C to remove nuclei and debris, collect supernatant and centrifuge again at 13,000 rpm for 30 min at 4 °C. The resulting supernatant was used as the soluble cytosolic fraction. Protein contents in cytosolic fraction were determined (see above). Following SDS-PAGE, Western blotting was performed to detect cytochrome-c release to cytosol using anti cytochrome-c pAb (Santa Cruz Biotechnology Inc., Santa Cruz, CA) and anti- β -actin mAb (Sigma)

2.18 Statistical analysis

The results are expressed as the mean ± standard deviation. All experiments were performed in triplicate. Significance was assessed with Student's t-test and was assumed for p-values<0.05.

Chapter 3

Effects of platinum nanoparticles on radiation-induced apoptosis in human lymphoma U937 cells

3.1 Summary

Since polyacrylic acid capped platinum nanoparticles (Pt-NPs) are known to have a unique ability to quench superoxide (O_2^-) and hydrogen peroxide (H_2O_2), the anti-oxidant activity of Pt-NPs against apoptosis induced by X-irradiation in human lymphoma U937 cells was investigated. DNA fragmentation assay, Annexin V-FITC/PI by flow cytometry and Giemsa staining revealed a significant decrease in apoptosis induced by 10 Gy, when cells were pre-treated with Pt-NPs in a dose-dependent manner. Pre-treatment with Pt-NPs significantly decreased X-rays-induced reactive oxygen species (ROS) production, Fas expression and loss of mitochondrial membrane potential as determined by flow-cytometry. Furthermore, western blot analysis also showed that the expression of cleaved caspase-3, Bid and cytosolic cytochrome-c were significantly reduced in Pt-NPs pretreated cells. Due to the catalase mimitic activity of Pt-NPs, these results indicate that pre-treatment of U937 cells with Pt-NPs significantly protect X-rays-induced apoptosis by inhibiting intracellular ROS (mainly H_2O_2), which plays a key role in the induction of apoptosis, because of no practical observation of intracellular O_2^- formation.

3.2 Specific research work

3.2.1 Effects of Pt-NPs on x-irradiation-induced apoptosis

To investigate whether Pt-NPs have an ability to protect against apoptosis induced by X-rays, U937 cells were exposed to (10 Gy) resulted in a large percentage of apoptotic cell death as manifested by DNA fragmentation which reaches up to 40.0 ± 5.0 %. This apoptotic percentage had decreased significantly in a dose dependent manner, when cells were pre-incubated with Pt-NPs at various concentrations (100, 200, 300 and 500 μM) for 24 h (Fig. 1A). Further, the intracellular uptake of Pt-NPs by U937 cells was confirmed by electron microscopy (Fig. 1B).

To observe the changes in cell morphology after treatment with Pt-NPs, X-rays alone and in combination of both were examined by Giemsa staining under a light microscope. When the cells were treated with the X-rays alone, typical morphological changes such as chromatin condensation and nuclear fragmentation occur (Fig 2D). The percentage of cells containing fragmented nuclei was significantly decreased after the combined treatment (Fig. 2E, F).

The flow cytometric analysis of the membrane changes indicative of different stages of apoptosis progression using annexin V-FITC and PI showed that the percentage of early apoptotic cells significantly decreased from 25.5 ± 2.0 % following X-rays treatment to 3.8 ± 2.0 % in the presence of 500 μM in U937 cells (Fig. 2G). On the other hand the percentage of secondary necrotic cells decreased from 0.7 ± 0.2 % to 0.5 ± 0.1 % respectively.

3.2.2 Suppression of intracellular ROS by Pt-NPs

We examined the effects of Pt-NPs on X-rays-induced ROS production in

U937 cells. Pt-NPs exert differential inhibition on X-rays induced ROS. The inhibitory effects of Pt-NPs on X-rays induced ROS; are plotted in (Fig. 3A, B & C). U937 cells were post-treated with X-rays with or without Pt-NPs at 500 μM for 24 h. Flow cytometry with DCFH-DA, APF and HPF staining were used to detect certain species of intracellular ROS production in treated cells [33]. A marked increase in the production of ROS was observed immediately after X-rays treatment in the cells. Pt-NPs at 500 μM concentration significantly inhibited X-rays induced ROS production.

3.2.3 Suppression of Fas receptor externalization by Pt-NPs

To examine the effects of Pt-NPs on Fas externalization, cells were exposed to X-rays with or without pre-incubation with 300 and 500 μM of Pt-NPs for 24 h. A significant decrease in Fas externalization was observed at 6 h after X-rays 9.2±0.2 % to 5.1±0.2 % and 4.6±0.2 % (Fig. 4A).

3.2.4 Assessment of intracellular caspase 8 activities

To determine whether the activated pathway to protect cells from apoptosis induced by X-rays is intrinsic or extrinsic, we studied the activity of caspase-8. Although the increase in activity is not significant in cells treated with X-rays alone, but in cells pre-treated with Pt-NPs, caspase-8 activities is significantly decrease approximately about 50 % (Fig. 4B).

3.2.5 Effects of Pt-NPs on the mitochondrial pathway

We determine whether the mitochondrial apoptotic pathway is related to decrease X-rays induced apoptosis by Pt-NPs. We found that the loss of mitochondrial membrane potential ($\triangle \Psi m$) which is the end point of apoptosis was significantly decreased in cells pre-treated with Pt-NPs for 24 h at 300 and 500 μM as compare to the

cells treated with X-rays alone (Fig. 5).

3.2.6 Effects of Pt-NPs on expression of apoptotic related proteins:

To investigate the mechanism of cell death, we also evaluated the expression level of apoptotic marker proteins as a result of X-rays and exposure to Pt-NPs (300 and 500 μM). Within the Bcl-2 family, the Western blotting revealed that the expression of t-Bid was significantly increased time dependently in alone x-irradiated treated U937 cells, whereas the pre-incubation with Pt-NPs resulted in decrease in its expression. However, no significant changes in the expression of Bax and Bcl-2 were observed after either treatment (Fig. 6A). Moreover, the Pt-NPs pre-treatment resulted in a significant decrease in cleaved caspase-3 expression compared to X-rays alone. Cytochrome-c was released in large amounts at X-rays (10 Gy) alone, although this was significantly decreased when cells pre-treated with Pt-NPs for 24 h (Fig. 6B).

3.3 Discussion

In this study we observed that Pt-NPs were able to suppress radiation-induced apoptosis in a concentration-dependent manner. Nanotechnology now has more importance for the development of new research to approach cancer treatment. [34]. The cytotoxic effects of platinum based drugs are well established therefore, it is very important to acknowledge the toxicity of platinum such as cisplatin, a platinum-based type of chemotherapy and is one of the cytotoxic agents commonly used in cancer chemotherapy. Cisplatin exerts its activity by interfering with transcription and other DNA-mediated cellular functions [2]. Further, it was reported that Pt-NPs have anti-tumor activity, affecting DNA integrity [35]. In contrast, the inhibitory effects of Pt-NPs on X-rays induced apoptosis were observed in the present study. However, this discrepancy with the findings of previous reports can be resolved by accounting the fact that the antitumor activity of Pt-NPs may be due to the lethal DNA damage effects caused by soluble Pt ion species, resulting in DNA strand breaks and formation of Pt–DNA complexes [4]. Furthermore, our results are consistent with the previous report, which showed that various sizes of Pt-NPs (<20, <100, >100 nm) exert no influence on proliferation or growth inhibitory effects indicating that Pt-NPs do not exhibit any serious cytotoxicity even at higher concentrations [4, 36].

X-rays induces oxidative injuries to DNA, membrane damage and cell death mostly due to the formation of intracellular ROS arising from radiolysis of water. X-rays initially generate $^{\cdot}OH$ which immediately recombine with another $^{\cdot}OH$ to form H_2O_2 ($^{\cdot}OH + {}^{\cdot}OH = H_2O_2$), whereas to form $O_2^{\cdot-}$ both aqueous electron and hydrogen atom react with O_2 ($H^{\cdot} + O_2 \rightleftarrows O_2^{\cdot-}$) and ($eaq^{\cdot} + O_2 \rightleftarrows O_2^{\cdot-}$), these free radicals contribute the indirect action of X-rays [37, 38]. Hydroxyl radical is the most important

ROS produced by X-rays, because of very high reaction rate constant and plays a crucial role in the induction of cell killing [39, 40] estimated by colony formation assay. This cell killing indicates mitotic cell death or reproductive cell death where cell death occurs after the cell division [41]. On the other hand cell death occurs before mitosis is called interphase death. During this phase mostly the cell death is characterized by apoptosis [42]. The prevention of radiation-induced apoptosis by an antioxidant is not simply associated with its scavenging ability for hydroxyl radicals and that the role of hydroxyl radicals in radiation induced apoptosis is relatively low [43, 44]. Therefore, in this study we focused on the scavenging activity of Pt-NPs on hydrogen peroxide.

Hydrogen peroxide has also been reported to induce apoptosis by Fas up-regulation [45]. Activation of Fas/FasL and their receptor on the cellular membrane implicated by X-rays induced apoptosis represent the involvement of extrinsic pathway [46]. Moreover, Fas/TNF-R1 activation can cause apoptosis via recruitment of the caspase cascade or via the mitochondria by activating caspase-8 and Bid [47, 48]. The intrinsic pathway involves the disruption of mitochondrial membrane, release of mitochondrial protein including cytochrome-c, action of Bcl-2 family members and p53 [49]. Both pathways ultimately trigger the effector caspase, and could be interconnected by the caspase-8 cleavage of Bid which activates the mitochondrial pathway [50, 45]. According to above discussion, it is considered that the mechanism of X-rays induced apoptosis may involve the activation of Fas on the cell membrane resulted from the changes in intracellular ROS, particularly peroxide (H_2O_2), induced by X-rays.

In the present study the result show positive correlation between the ROS scavenging activity of Pt-NPs and their anti-apoptotic effects. Because Pt-NPs significantly inhibited X-rays induced peroxide (H_2O_2) formation, which is well known

as one of the most reactive free radical involve in X-rays induced apoptosis [51]. This finding indicates that ROS scavenging activity of Pt-NPs is involved in their anti-apoptotic effects. It was reported that Pt-NPs protects against UV-induced inflammation by decreasing ROS production and inhibit apoptosis in HaCaT keratinocytes [7]. Several other studies also reported the ROS scavenging activity of Pt-NPs both vitro [37, 52] and in-vivo [7, 9, 53]. Recently our group has demonstrated that treatment with 100 μM of Pt-NPs was able to reverse the hyperthermia induced apoptosis in the same cell line [7]. While, higher concentration of Pt-NPs was used in this study. The reason behind this discrepancy between two studies is well known that the mechanism involved in apoptosis induced by X-rays is different from hyperthermia [39].

Caspases, a family of intracellular cysteine proteases, are also an important executor of apoptosis and play a central role in morphological changes associated with apoptosis. In all the caspases, caspase-3 is the most common executor of apoptosis whereas; caspase-8 is known to be located at upstream in the caspase cascade; which is capable of inducing the release of cytochrome-c in the cytosol from the damaged mitochondria [54]. Another family of proteins, the Bcl-2 family, is involved in pro or anti apoptotic process by interacting with the mitochondria [55]. Bid a pro-apoptotic Bcl-2 family member containing BH3 domain, can be cleaved by caspase-8, and the cleaved Bid, the carboxyl-terminal fragment, translocate to the mitochondria to induce the release of cytochrome-c [56, 57].

This study affirmed the previous findings that irradiation activates caspase-3 and caspase-8 and induces loss of MMP associated with the release of cytochrome-c to the cytosol and decreased Bid. Our results demonstrated the reduction in Fas expression

and restoration of the decreased MMP in the presence of Pt-NPs. No significant changes in the expression of Bcl-2 family proteins Bax and Bcl-2 were observed. However, Pt-NPs treatment significantly inhibited the t Bid (activated form of Bid) and release of cytochrome-c from the cytosol induced by X-rays. Furthermore, our data clearly showed the caspase-3 activation by x-irradiation and its inhibition in the presence of Pt-NPs. Therefore, taken together these findings confirmed the involvement of mitochondrial caspase pathway and its modulation by intracellular peroxide in X-rays induced apoptosis.

3.4 Conclusion

In summary we conclude that Pt-NPs suppresses X-rays induced apoptosis mainly by scavenging of ROS which inhibit the activation of Fas receptor so that the activity of caspase-8 and caspase-3 were decreased and does not allow to change the mitochondrial membrane potential in result the level of cytochrome-c in cytosol remain lower which ultimately inhibit X-rays induced apoptosis (Fig. 7).

3.5 Figures and Illustrations

Fig. 1A

Effects of Pt-NPs on X-rays induced DNA fragmentation.

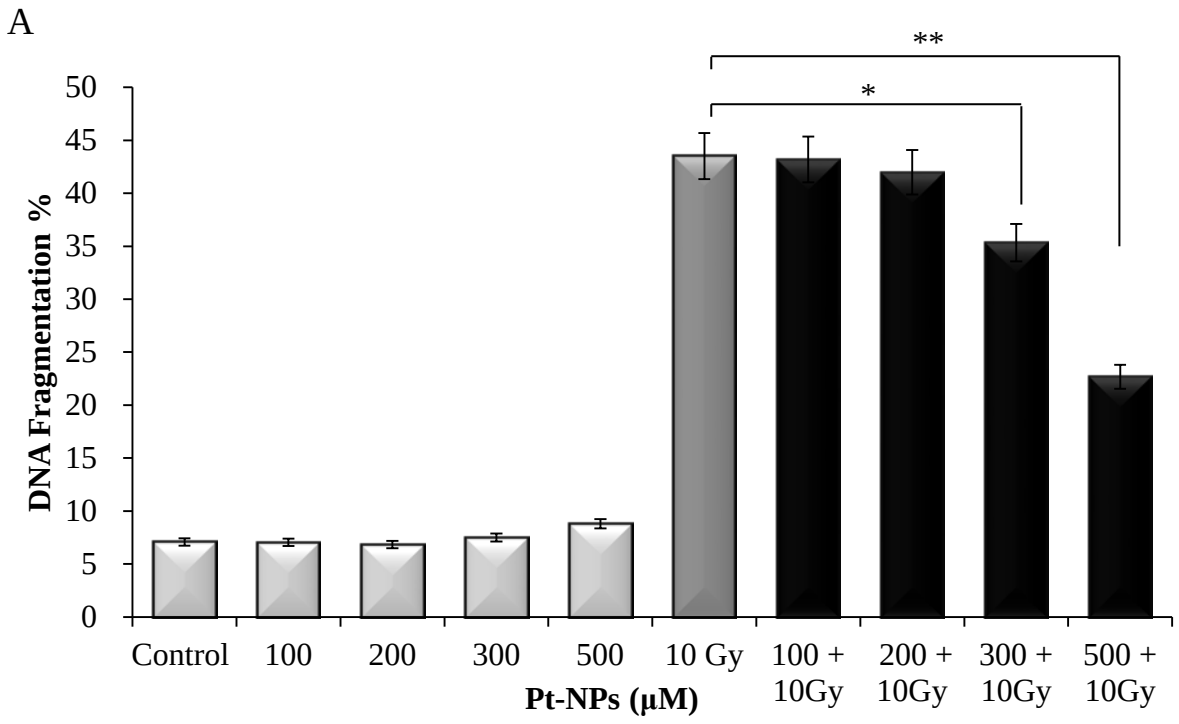

Cells were post-treated with X-rays at a dose of 10 Gy with or without pre-incubation with Pt-NPs at different concentrations for 24 h. DNA fragmentation assay was carried out at 6 h post X-rays exposure. Data are presented as mean $\pm$ SD. *P < 0.01, **P < 0.005. Data shown are representative of three independent experiments

Fig. 1B

Intracellular uptake of Pt-NPs by U937 cells were determined by electron microscopy at high magnification (500.0nm).

B

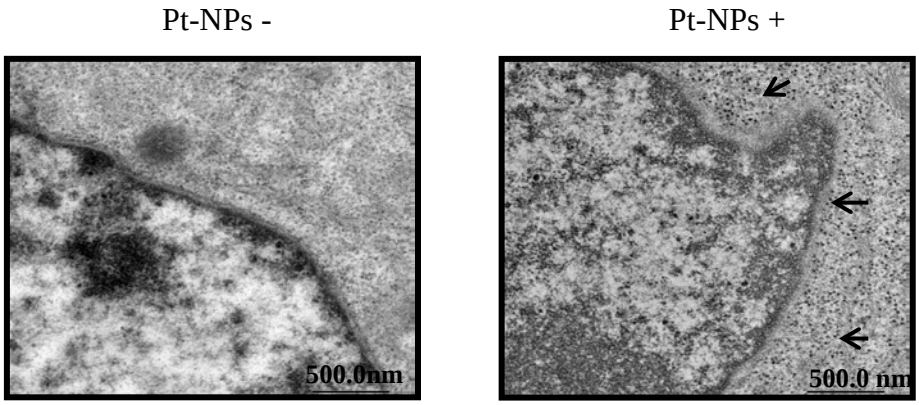

The black dots spread in the cell are Pt-NPs, some Pt-NPs were pointed out with black arrow heads.

Fig. 2A - F

Assessment of morphological changes in X-rays induced apoptosis.

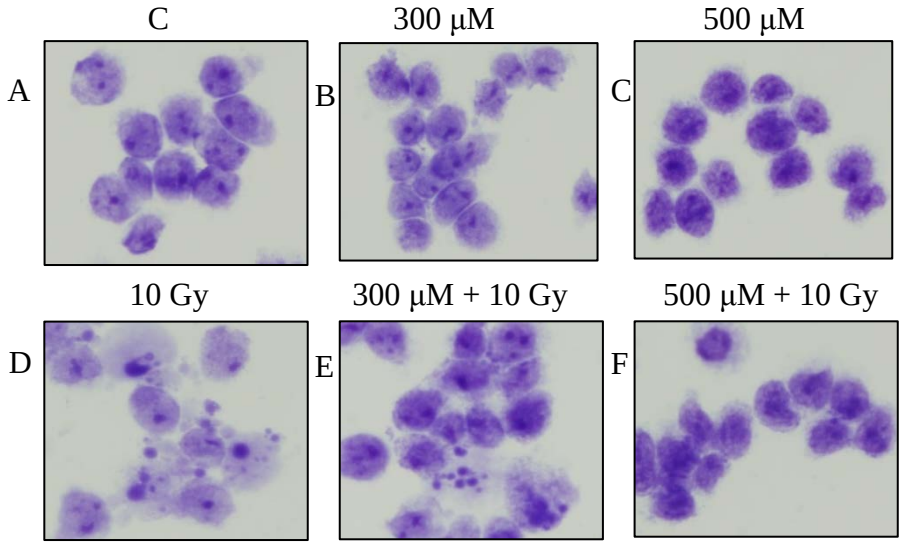

U937 cells were treated with X-rays (10 Gy) with or without pre-treatment with Pt-NPs for 24 h, and the cells were harvested 6 h after X-rays treatment. Apoptotic features of U937 cells in response to the combined treatment with X-rays and Pt-NPs. Sign of apoptosis were detected by Giemsa staining and then examined under a microscope at x400 magnification.

Fig. 2G

Effects of Pt-NPs on X-rays induced early apoptosis and secondary necrosis.

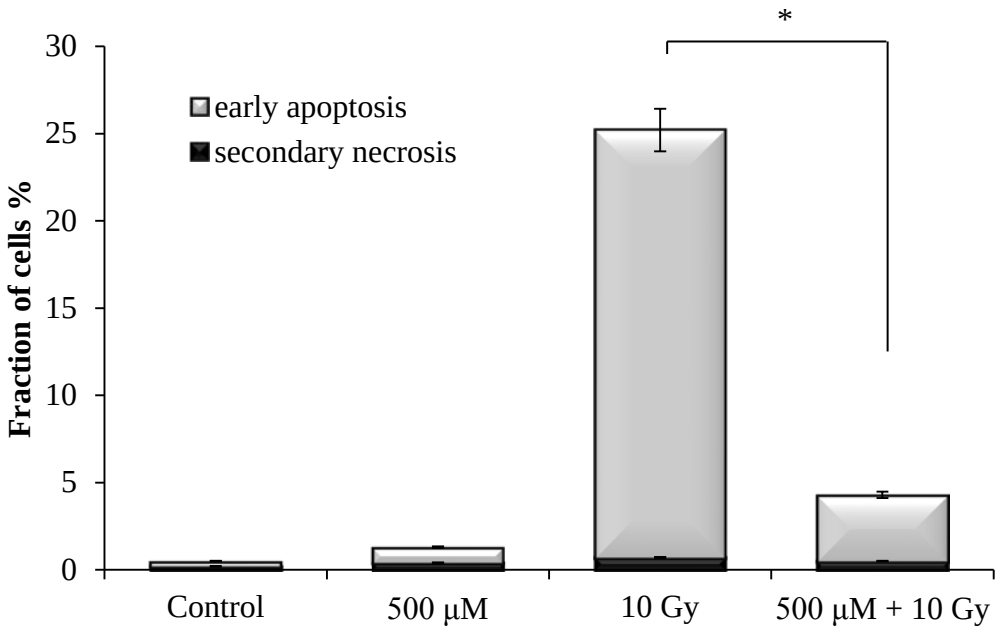

Cells were treated with X-rays with or without Pt-NPs (500 μM) for 24 h. Percentage of early apoptosis and secondary necrosis were analyzed 6 h after X-rays treatment by flow cytometry. Data are presented as mean ± SD. *P < 0.005. Data shown are representative of three independent experiments

Fig. 3A, B & C

Effects of Pt-NPs on X-rays induced intracellular ROS production.

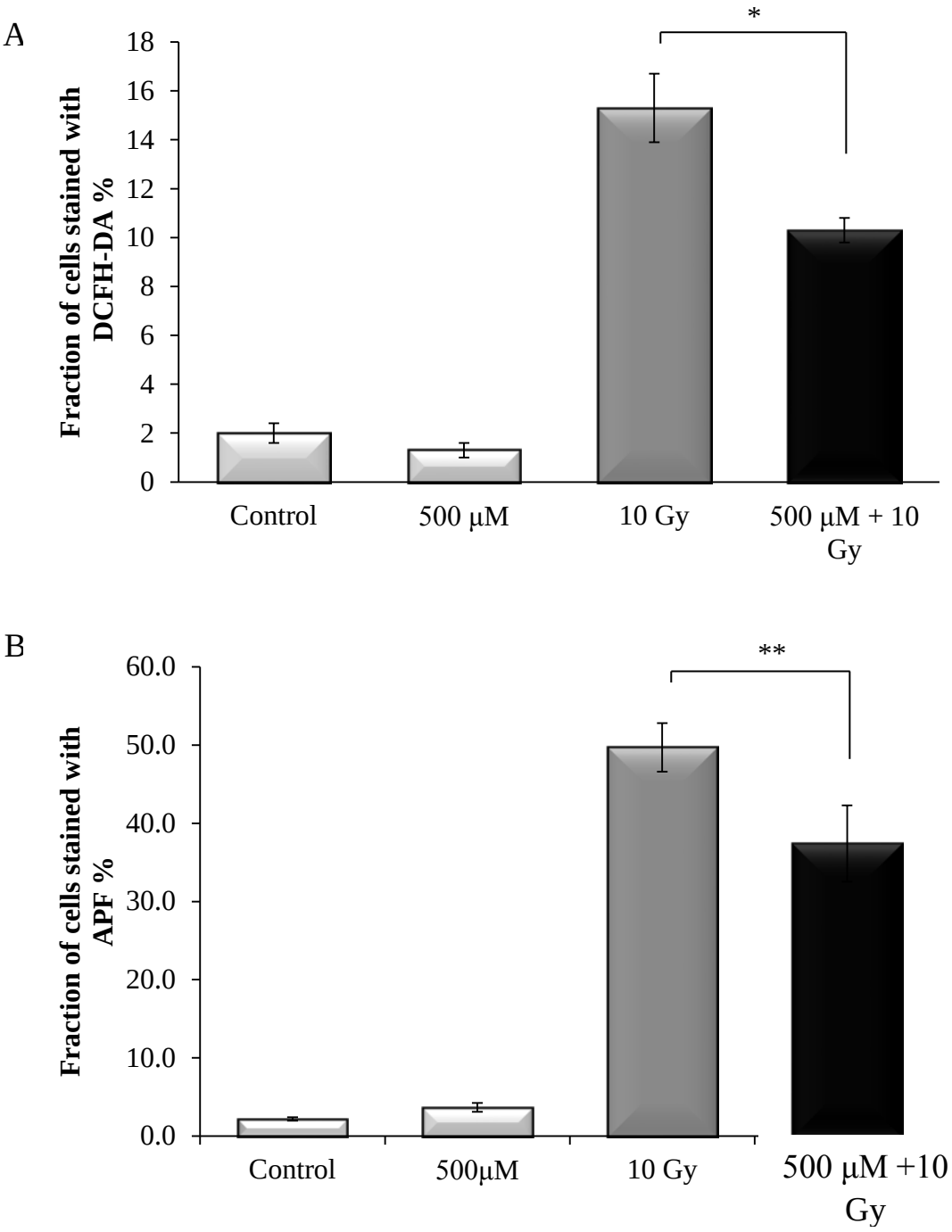

C

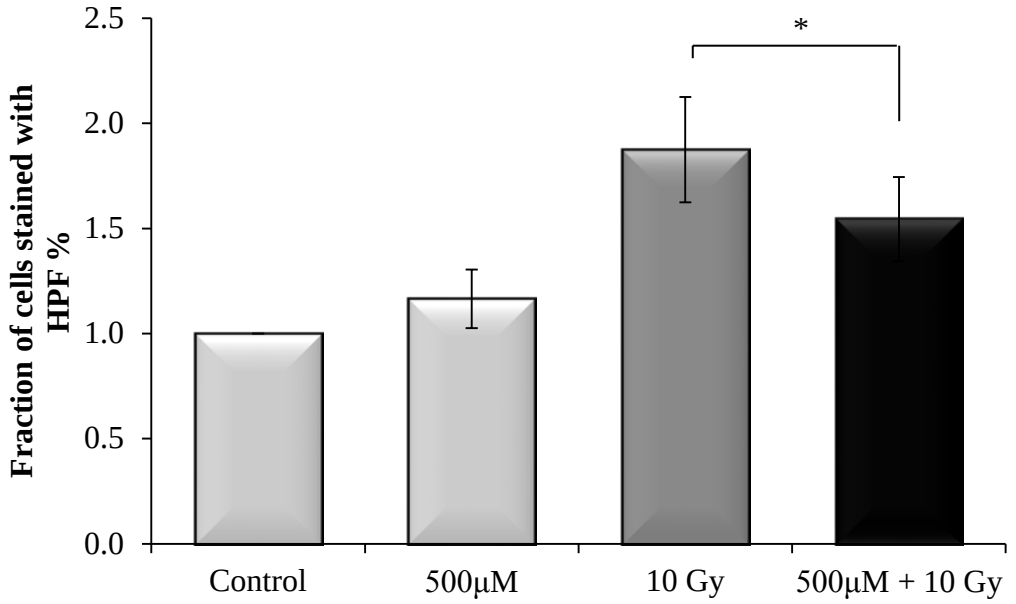

The percentages of cells with elevated some species of ROS (H_2O_2, $^{\cdot}OH$, NO, OCl^-, ONOO) were analyzed immediately after X-rays with flow cytometry. The results are presented as mean ± SD. *P < 0.05, **P < 0.005. Data shown are representative of three independent experiments

Fig. 4A

Effects of Pt-NPs on X-rays induced Fas externalization.

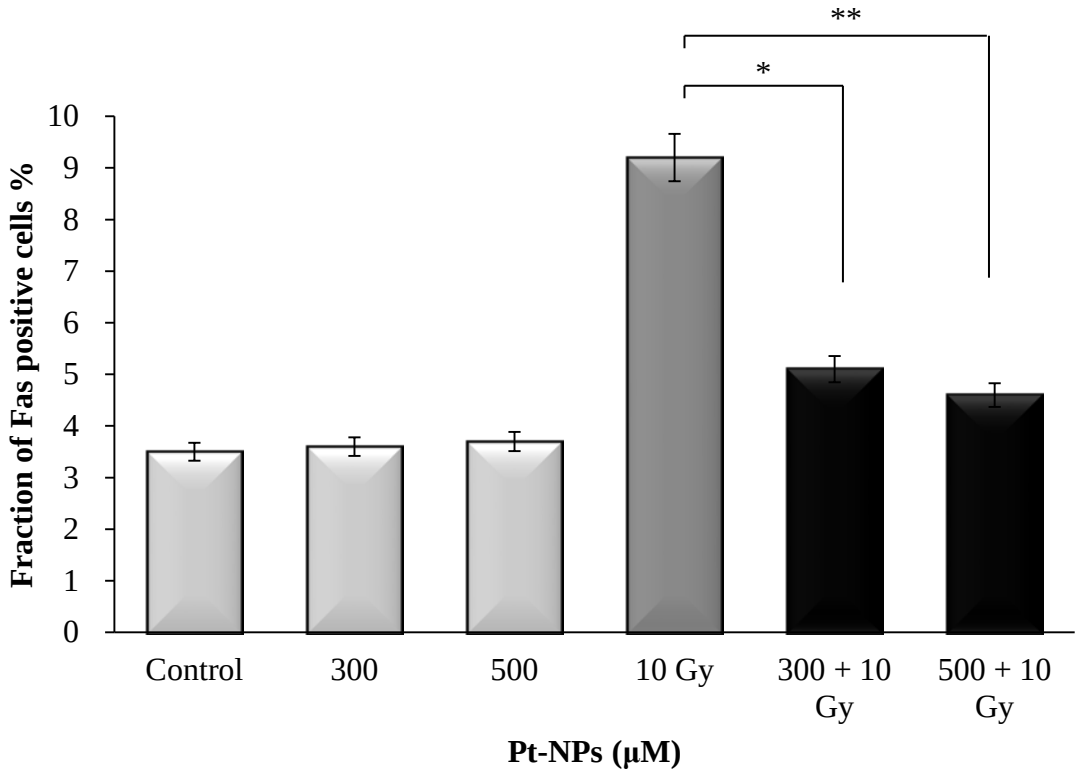

U937 cells were pre-treated with Pt-NPs (500 μM) for 24 h and then harvested 6 h after X-rays (10 Gy). Then the fraction of cells externalization Fas was analyzed by Flow cytometry using anti-Fas FITC-conjugated antibody. Data are presented as mean ± SD. *P < 0.01, **P < 0.005. Data shown are representative of three independent experiments

Fig. 4B

Activation of caspase-8 in U937 cells

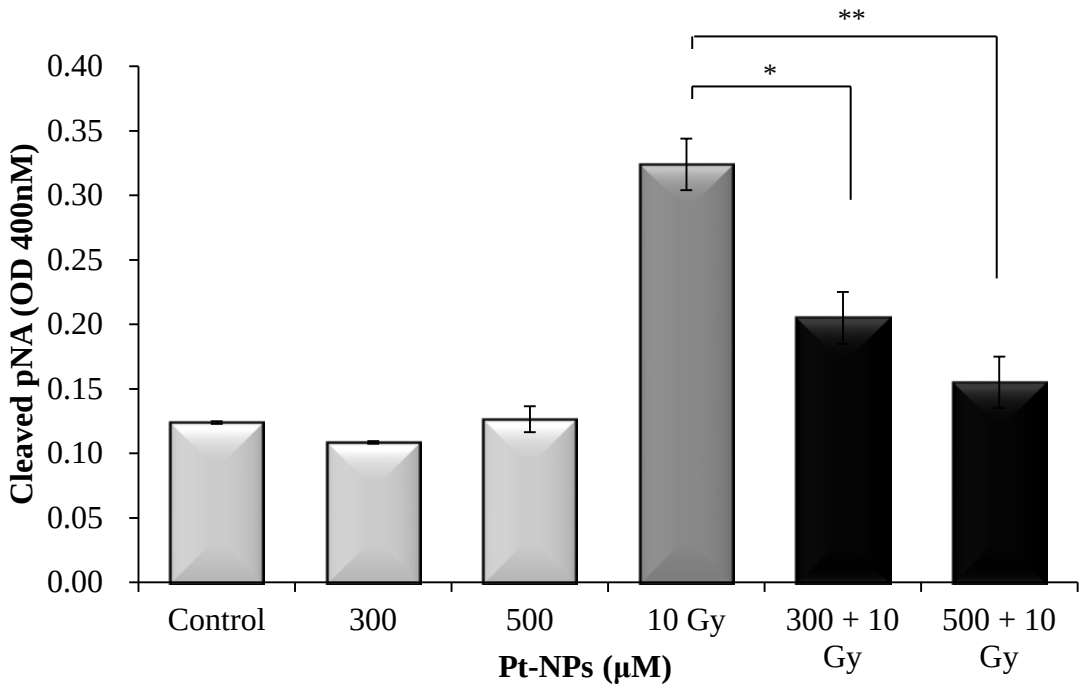

Activation of caspase-8 in U937 cells with and without pre-treatment with Pt-NPs was measured by FLICE/Caspase-8 colorimetric protease kit. The results are presented as mean $\pm$ SD. *P < 0.05. Data shown are representative of three independent experiments

Fig. 5

Effects of Pt-NPs on X-rays induced loss of MMP.

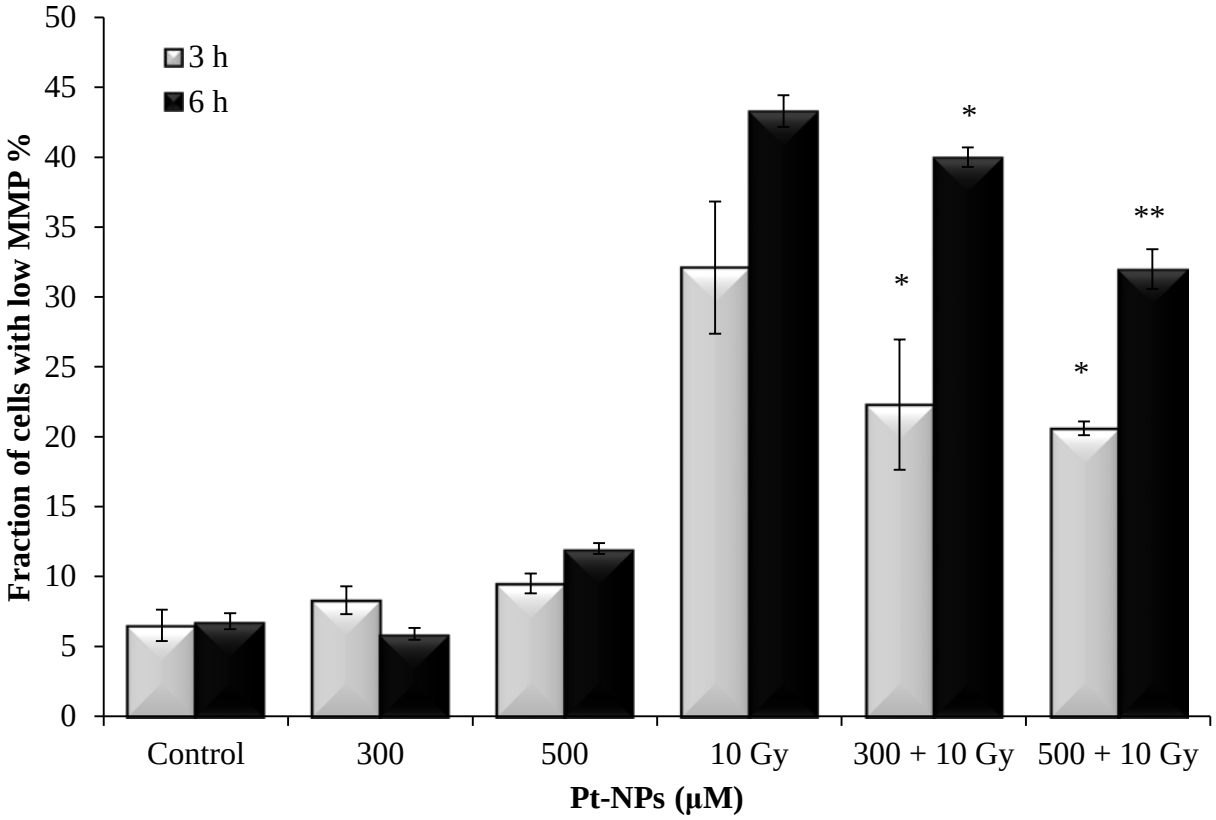

Cells were treated with X-rays (10 Gy) with or without 24 h pre-treatment with (300 and 500 µM) of Pt-NPs. At 3 h and 6 h following different treatments, the percentage of MMP loss was analyzed by Flow cytometry using TMRM staining. The results are presented as mean $\pm$ SD. *P < 0.05, **P < 0.005. Data shown are representative of three independent experiments

Fig. 6A & B

Western blotting for changes in the expression of apoptosis related proteins.

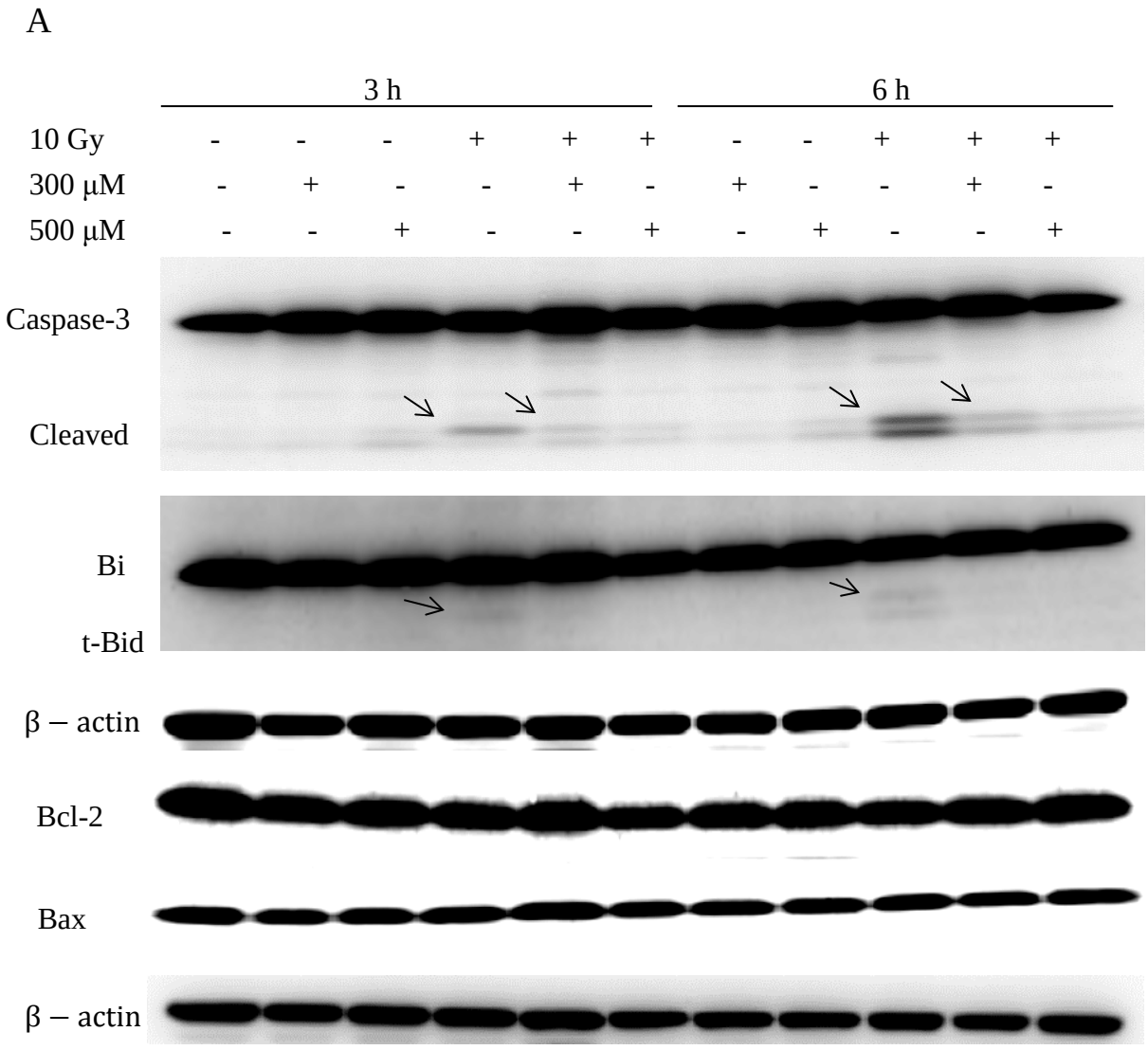

B

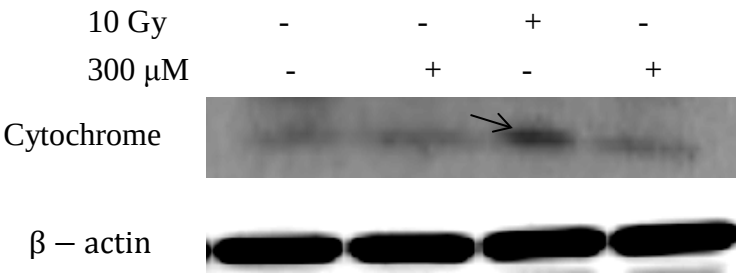

Cells were pre-incubated with or without Pt-NPs (300 and 500 μM) for 24 h and then harvested 3 and 6 h after X-rays. (A) Western blot analysis of Bcl-2 family and caspase-3. (B) Western blot analysis of cytosolic cytochrome c. Data shown is representative of three independent experiments

Fig. 7

Graphical scheme of the pathways involved in the protective effects of Pt-NPs against ionizing radiation induced apoptosis in U937 cells

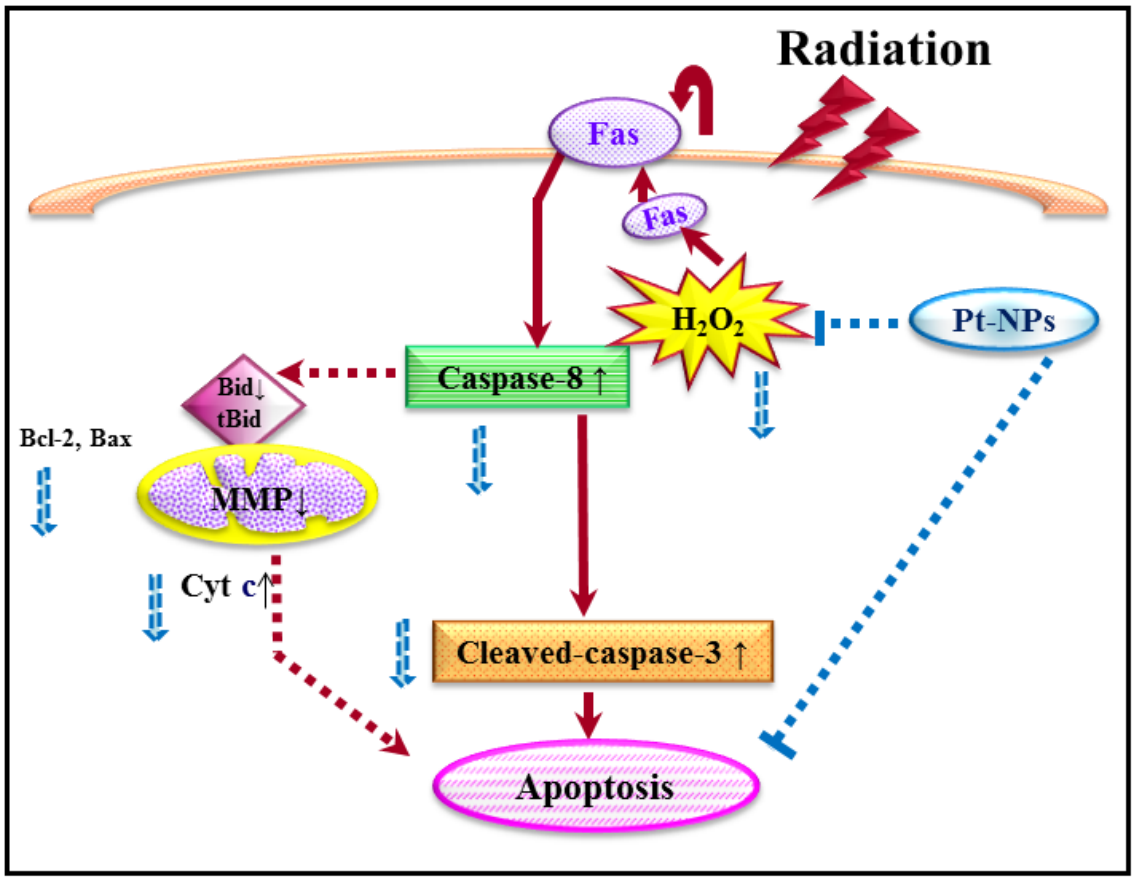

Chapter 4

Platinum nanoparticles prevent from Helium based cold atmospheric plasma-induced apoptosis via suppression of ROS generation

4.1 Summary

Plasma is generated by ionizing gas molecules. Helium (He)-based cold atmospheric plasma (CAP) was generated using a high-voltage power supply with low-frequency excitation (60 Hz at 7 kV) and He flow at 2 L/min (Fig. 8). Platinum nanoparticles (Pt-NPs) have an anti-tumor activity and the ability to scavenge superoxides and peroxides. These features make them useful for the protection against oxidative stress-associated pathologies. However, the combined use of Pt-NPs with other therapeutic modalities remains unclarified. Here, the effects of Pt-NPs on He-CAP-induced apoptosis and the underlying mechanism were examined. The results indicate that the Pt-NPs substantially scavenge He-CAP-induced superoxides and peroxides and inhibit all the pathways involved in apoptosis execution. This might be due to the SOD/catalase mimetic effects of Pt-NPs. These results showed that the Pt-NPs can induce He-CAP desensitization.

4.2 Specific research work

4.2.1 Effects of He-CAP on cell viability and apoptosis

Human lymphoma U937 cells were treated with He-CAP for 1, 2, 3 and 4 min then trypan blue exclusion dye assay was performed to assess the viability of cells at 12, 18 and 24 h. As shown in (Fig. 9A) dose and time-dependent decreased in the viability of cells was observed in the cells treated with He-CAP as compare to control. Furthermore, to determine the effects of He-CAP on apoptosis, the cells were subjected to annexin V-FITC and PI double staining. Flow cytometry revealed that the He-CAP treatment significantly increased the percentage of apoptotic cells in a dose and time-dependent manner (Fig. 9B). Since, increased apoptosis was observed at He-CAP treatment for 4 min, we used He-CAP 4 min exposure in the subsequent experiments.

4.2.2 Effects of Pt-NPs on He-CAP-induced apoptosis

To investigate whether Pt-NPs have an ability to protect against apoptosis induced by He-CAP, U937 cells were treated with He-CAP for 4 min in the presence or absence of Pt-NPs at 300 μM, and the trypan blue exclusion dye was used to assess cell viability. As shown in (Fig. 9C) the percentage of dead cells was significantly decreased upon combine treatment at 24, 48 and 72 h compare to the cells treated with He-CAP alone. Further, to confirm the growth of U937 cells, U937 cells were counted under a microscope using a haemocytometer at 24, 48 and 72 h after post-treatment. Cell count in combine treatment showed significantly increased in no of cells as compare to alone He-CAP treated cells (Fig. 9D).

U937 cells treated with He-CAP resulted in a large percentage of apoptotic cell death as manifested by the increased in the percentage of DNA fragmentation, a hallmark

of apoptosis which reaches up to 28.0 ± 2.0 %. This increase in the DNA fragmentation was significantly decreased, in the presence of Pt-NPs at 300 μM (Fig. 10A).

Furthermore, to distinguish between the early and late phase of apoptosis, cell were subjected to annexin V-FITC and PI double staining. The flow cytometry revealed that the percentage of early apoptotic cells decreased from 13.5 ± 1.0 % following He-CAP treatment to 7.0 ± 1.0 % in the presence of Pt-NPs at 300 μM. On the other hand the percentage of secondary necrotic U937 cells significantly decreased from 40.5 ± 3.0 % to 5 ± 1.0 %, respectively (Fig. 10B). Moreover, giemsa staining showed that typical morphological changes related to apoptosis such as chromatin condensation and nuclear fragmentation were more prominent in the cells treated with He-CAP alone (Fig. 10C (iii)). However, these morphological changes were significantly decreased in the presence of Pt-NPs. (Fig. 10C (iv)).

4.2.3 Effects of Pt-NPs on He-CAP-induced cell cycle distribution

U937 cells were treated with He-CAP in the presence or absence of Pt-NPs at 300 μM. The effects of combined treatment on cell cycle distribution are shown in (Table. 1) the percentage of cells in the sub G1 was increased following He-CAP treatment. However, in the combined treatment the percentage of cells in sub G1 significantly decreased from 24.0 ± 2.5 to 9.8 ± 0.5 respectively, than the He-CAP alone treated cells. This increase in the percentage of sub G1 population was determined by a decrease of cells in the G1 and G2/M phases, which may be caused by apoptosis.

4.2.4 Effect of Pt-NPs on He-CAP-induced reactive oxygen species (ROS) generation

Because, ROS generation plays an important role in He-CAP induced apoptosis, we examined the effects of Pt-NPs on He-CAP-induced ROS production in U937 cells.

The effects of Pt-NPs on He-CAP induced ROS generation; are plotted in (Fig. 11A & B). U937 cells were pre-treated with Pt-NPs at 300 μM for 3 and 6 h before He-CAP treatment. Flow cytometry with DCFH-DA and HE staining was used to detect certain species of intracellular ROS production in treated cells. A marked increase in the production of ROS was observed immediately after He-CAP treatment in the cells. However, Pt-NPs at 300 μM significantly inhibited He-CAP-induced ROS production ($p<0.05$ *vs* He-CAP alone).

4.2.5 Measurement of mitochondrial membrane damage

To assess the involvement of the mitochondrial apoptotic pathway in the inhibition of He-CAP-induced apoptosis by the combined treatment, the effects of the treatments on mitochondrial membrane potential (MMP) were evaluated. It was found that the MMP loss ($\Delta\Psi m$), which is the end point of apoptosis was significantly decreased in the cells treated with Pt-NPs immediately before He-CAP treatment at 300 μM as compare to the cells treated with He-CAP alone (Fig. 12A and B). The percentage of MMP loss was analyzed by Flow cytometry using TMRM staining.

4.2.6 Effect of Pt-NPs on intracellular $[Ca^{2+}]_i$ levels

Changes in $[Ca^{2+}]_i$ levels were assessed by flow cytometry. The results showed that intracellular $[Ca^{2+}]_i$ levels were increase by approximately twentyfold of the basal levels following He-CAP treatment alone. On the other hand, Pt-NPs significantly suppressed the He-CAP- induced increased $[Ca^{2+}]_i$ level (Fig. 13).

4.2.7 Expression of apoptosis-related proteins

Western blot analysis revealed that the increased expression level of the pro-apoptotic Bcl-2 family protein, truncated Bid (tBid, an active form of Bid) was

observed following He-CAP treatment alone. However, in the presence of Pt-NPs the expression level of tBid was markedly decreased. While, no significant changes in the expression levels of pro-apoptotic Bax and anti-apoptotic Bcl-2, Bcl-xl were observed after treatment either with He-CAP alone or in combination with Pt-NPs (Fig. 14A).

Caspases play a key role in the apoptosis and considered as the main executioner of apoptosis signaling pathways. The effects of combined treatment on the activation of caspase-3 were evaluated. Following He-CAP treatment, the expression level of the active form of caspase-3 (cleaved caspase 3) was markedly increased. However, the combined He-CAP treatment with Pt-NPs strongly suppressed the expression of the caspase-3 active form. Furthermore, to confirm the activation of the caspase cascade, the expression level of the x-linked inhibitor of the apoptosis protein XIAP was determined by western blot analysis. Since XIAP has been known as the potent inhibitor of caspase-3 and stop apoptotic cell death, it was found that following combined treatment, the XIAP expression level was higher than that following the He-CAP treatment alone (Fig. 14B).

4.2.8 Effect of Pt-NPs on He-CAP-induced FAS externalization and caspase-8 activation

The Fas receptor is a death receptor on the surface of cells that leads to one of the apoptotic pathways, i.e; the extrinsic pathway, through DISC assembly and subsequent caspase-8 activation. The Fas externalization and caspase-8 activity were detected in U937 cells at 18 h after He-CAP treatment. The results showed that Pt-NPs significantly suppressed He-CAP-induced Fas externalization and caspase-8 activation (Fig. 15A & B).

4.2.9 Effects of Pt-NPs on He-CAP-induced apoptosis in other cancer cell lines

The effects of Pt-NPs in combination with He-CAP were also determined in other cancer cell lines namely Molt-4, Jurkat, Hela and HCT-116 cells. In Hela and HCT-116 cells the percentages of early apoptosis and secondary necrotic cells after 24 h were significantly decreased in the presence of Pt-NPs 300 μM then in He-CAP treatment alone (Fig. 16A and B).

Similarly, in Molt-4 and Jurkat cells PI staining 6 h after He-CAP treatment showed a significant increase in the percentage of apoptotic cells in the absence of Pt-NPs, which was inhibited in the presence of Pt-NPs (Fig. 17A & 18A). In addition, trypan blue assay at 6 h also showed the protective effects of Pt-NPs on He-CAP-induced apoptosis (Fig. 17B & 18B).

4.3 Discussion

In this study, it was demonstrated that treatment with Pt-NPs suppressed He-CAP-induced apoptosis. Therefore, the assumptions regarding the usefulness of Pt-NPs in combination with He-CAP seem to be true. It has been demonstrated that the electromagnetic, optical, and catalytic properties of noble-metal nanocrystals are strongly influenced by their shape and size [58, 59]. However, the toxicity of platinum based compounds is also well established. [60]. One such commonly used cytotoxic agent in cancer chemotherapy is cisplatin, which exerts its effects by interfering with transcription and other DNA-mediated cellular functions [2]. Further, it was reported that Pt-NPs are capable of inducing DNA damage and p53-mediated growth arrest [4]. Considering the facts mentioned above, one may speculate that the combined treatment of Pt-NPs with He-CAP may enhance the effect of He-CAP on inducing apoptosis. However, our study showed that Pt-NPs inhibit He-CAP-induced apoptosis.

Several studies concerning the antioxidant effects of Pt-NPs showed that Pt-NPs can reverse the hyperthermia (HT) induced apoptosis through the suppression of all the involved micro-molecular pathways particularly *via* suppression of intracellular ROS [3], as well as protects mouse RAW24.7 macrophages from LPS-induced inflammation by scavenging ROS [36]. The Pt-NPs used in this study were believed to quench ROS, owing to their large surface area of smaller particles [1, 61].

Growing evidence indicates that CAP has the potential to be a safe anticancer therapy that can be used for selective killing of various cancer cells, such as breast [62] liver [63] ovarian [64] leukemia [65]. It is well known that He-CAP-induced cell death is mainly mediated by the generation of ROS, including $^{\cdot}OH$, H_2O_2 and O_2^{-}. CAP-induced ROS (or their reaction products) in the liquid phase, then diffuse through the

plasma membrane or react with the plasma membrane to produce intracellular ROS through lipid peroxidation [66, 67], resulting in the release of growth factors in proliferating cells [68], which cause damage to intracellular components or promote or inhibit of intracellular signaling pathways [69, 70] and DNA damage in cancer cell lines [27, 28]. It was reported that H_2O_2 and O_2^- are the major species involved in the apoptosis and cell death induced by CAP. In this study, it was demonstrated that treatment with Pt-NPs protects against He-CAP-induced apoptosis in U937 cells, which is mainly due to the scavenging effect of Pt-NPs on He-CAP-induced H_2O_2 and O_2^- generation, suggesting the SOD/catalase mimetic activity of Pt-NPs. These findings are consistent with the observation that treatment of cells with H_2O_2 and O_2^- scavengers can reverse the biological effects of plasma [71]. Because, He-CAP-induced extracellular ROS, might be scavenged immediately in the presence of Pt-NPs, thereby preventing its further interaction with the plasma membrane, resulting in the reversal of He-CAP-induced effects in U937 cells. Therefore, the role of Pt-NPs or He-CAP at the cell membrane level might exist and also the intracellular effects on the protein level may prevent cells from undergoing He-CAP-induced apoptosis.

ROS activate the intrinsic apoptotic pathway due to their interaction with proteins with the mitochondrial permeability transition complex [72]. In addition, ROS specifically H_2O_2 has also been reported to induce apoptosis by Fas up-regulation [45]. Furthermore, FAS/TNF-R1 can cause apoptosis via the direct recruitment of the caspase cascade or via the mitochondria by activating caspase-8 and Bid [47, 48]. The intrinsic pathway involves the disruption of the mitochondrial membrane, release of mitochondrial proteins including cytochrome-c, increase in $[Ca^{2+}]_i$, activation of Bcl-2 family members and p53 [49]. These two apoptotic pathways ultimately trigger the

effector caspase which results in cellular shrinkage and DNA fragmentation which could be interconnected by the caspase-8-mediated cleavage of Bid, which triggers the activation of the mitochondrial pathway. In this study, it was demonstrated that the fraction of cells with decreased MMP were substantially increased following the He-CAP treatment with the concurrent increases in $[Ca^{2+}]_i$ and activation of caspase-3. These findings suggest the involvement of the caspase-dependent mitochondrial pathway in the He-CAP-induced apoptosis in U937 cells. Moreover, the involvement of the extrinsic pathway was confirmed from the increased FAS and caspase-8 activation following He-CAP treatment, which might result from the changes in intracellular ROS generation. Furthermore, increased Bid activation was observed following He-CAP treatment. Bid can be cleaved by caspase-8 and the cleaved Bid as the carboxyl-terminal fragment translocates to the mitochondria to induce the release of cytochrome-c [54, 55]. Previously, in the HeLa cell line, it was demonstrated that the atmospheric-pressure plasma jet-induced apoptosis was mediated through the mitochondria-dependent pathway via the generation of free radicals, without any involvement of death receptors [73]. In contrast, our findings showed the involvement of both the intrinsic and extrinsic pathways and the Ca^{2+}-dependent pathway of apoptosis following He-CAP treatment in U937 cells. This discrepancy is may be due to the induction of different cellular pathways induced by CAP depending on the target and cell line used. Therefore, it can be assumed that the caspase-8-mediated activation of Bid also contributed in the mitochondrial pathway during apoptosis induced by He-CAP treatment in U937 cells. However, in the presence of Pt-NPs the suppression of both the extrinsic and intrinsic pathways was observed via the reduction in Fas expression level and restoration of the decreased MMP. Taken together, this study showed positive correlation between the

ROS scavenging activity of Pt-NPs and their anti-apoptotic roles against He-CAP-induced apoptosis.

4.4 Conclusion

In conclusion, this study is the first to demonstrate that Pt-NPs mainly scavenged He-CAP-induced ROS, resulting in the inhibition of the ROS-mediated release of $[Ca^{2+}]_i$ and activation of the Fas receptor, so that the activity of caspase-3 and caspase-8 was decreased, which prevent the loss of MMP and ultimately inhibit He-CAP-induced apoptosis (Fig. 18).

4.5 Table, Figures and Illustrations

Fig. 8

Helium based cold atmospheric plasma (He-CAP) device

Fig. 9

He-CAP-induced cell death in U937 cells.

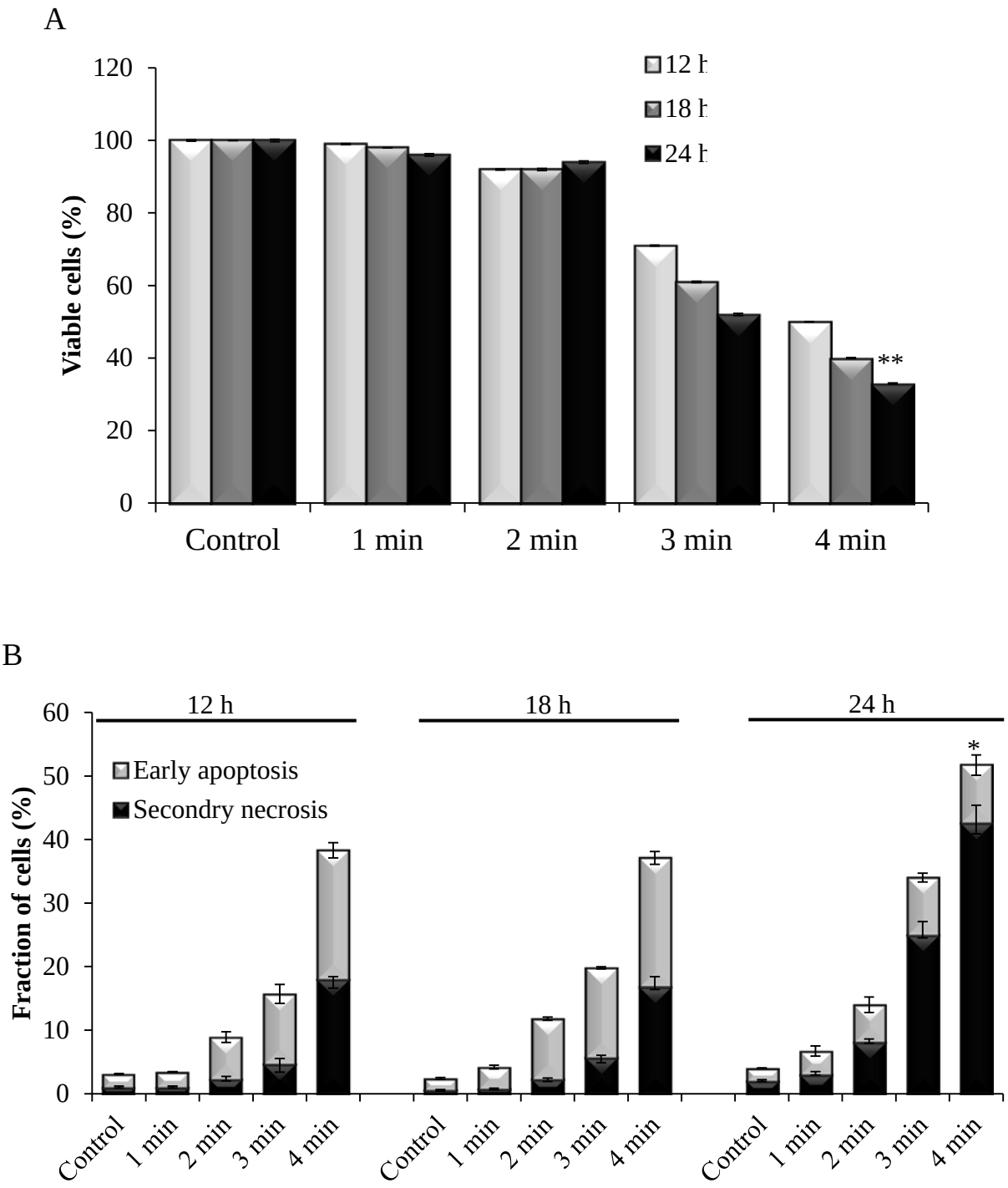

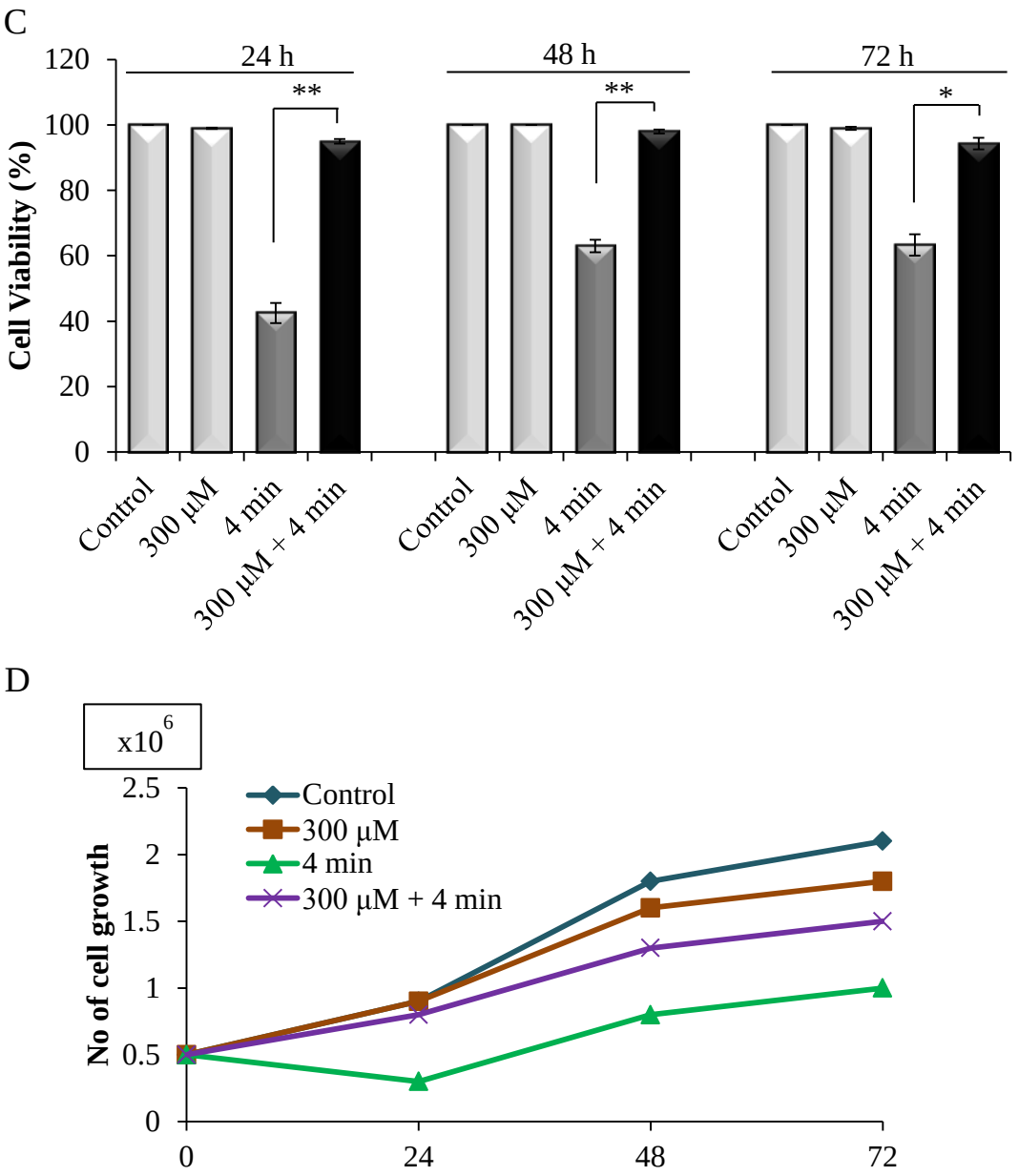

Cells were treated with He-CAP at a dose of (1, 2, 3 and 4 min). (A) Cell viability assessment and (B) annexin V-FITC/PI assay were carried out at 12, 18 and 24 h after He-CAP treatment. (C) Viability of cells in the presence or absence of Pt-NPs. (D) Cell growth or cell proliferation. Cells were harvested after treatment with He-CAP in the presence or absence of Pt-NPs. The number of cells/ml was counted at 24, 48 and 72 h to assess proliferation. Data are presented as mean ± SD. *P≤0.05, **P≤0.005. Data shown are representative of five independent experiments.

Fig. 10:

Effect of Pt-NPs on apoptosis induced by He-CAP in U937 cells.

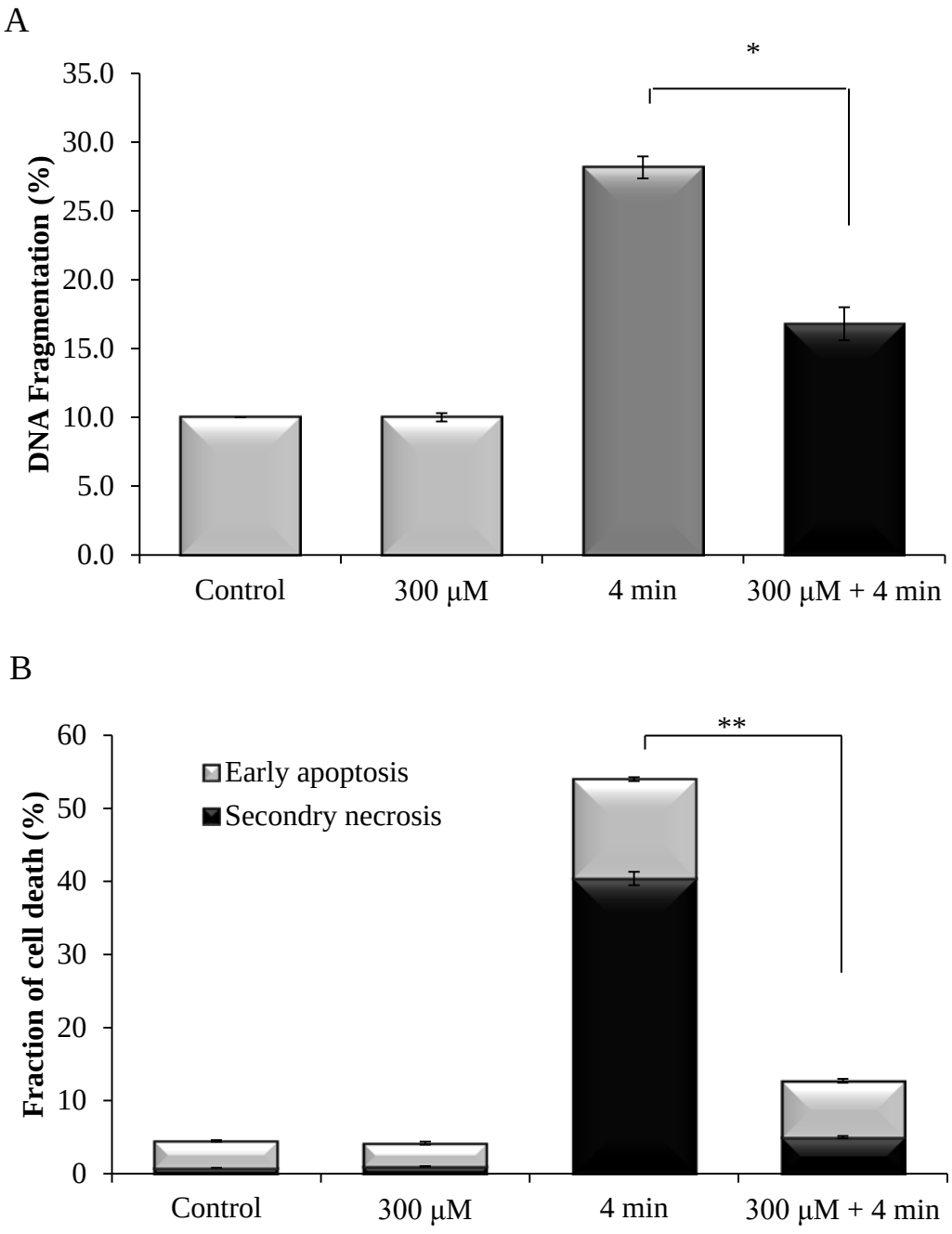

C

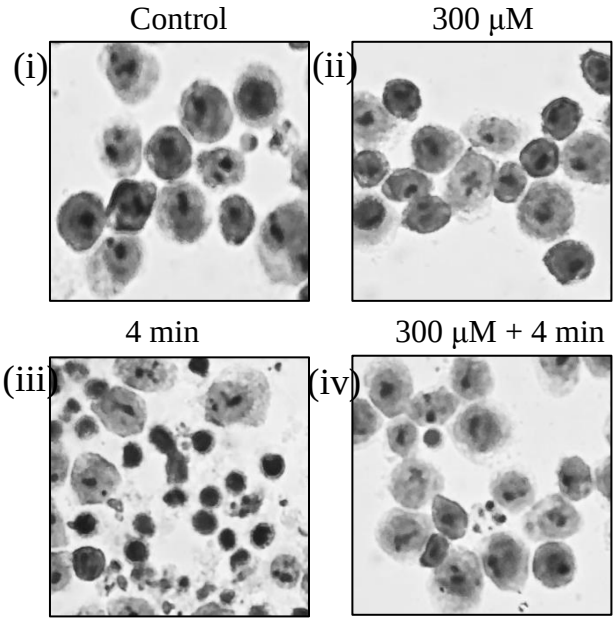

(A) DNA fragmentation assay (B) Percentages of early apoptotic and secondary necrotic cells were analyzed 24 h after He-CAP treatment with or without Pt-NPs by flow cytometry. Data are presented as mean ± SD. *P≤0.05, **P≤0.005. Data shown are representative of five independent experiments. (C) Morphological features of apoptosis in U937 cells following treatment with He-CAP in the presence or absence of Pt-NPs; cells were harvested 24 h after treatment, signs of apoptotic features in response to He-CAP were detected by Giemsa staining and then examined under a microscope at x400 magnification.

Fig. 11

Effect of Pt-NPs on He-CAP-induced ROS formation in U937 cells.

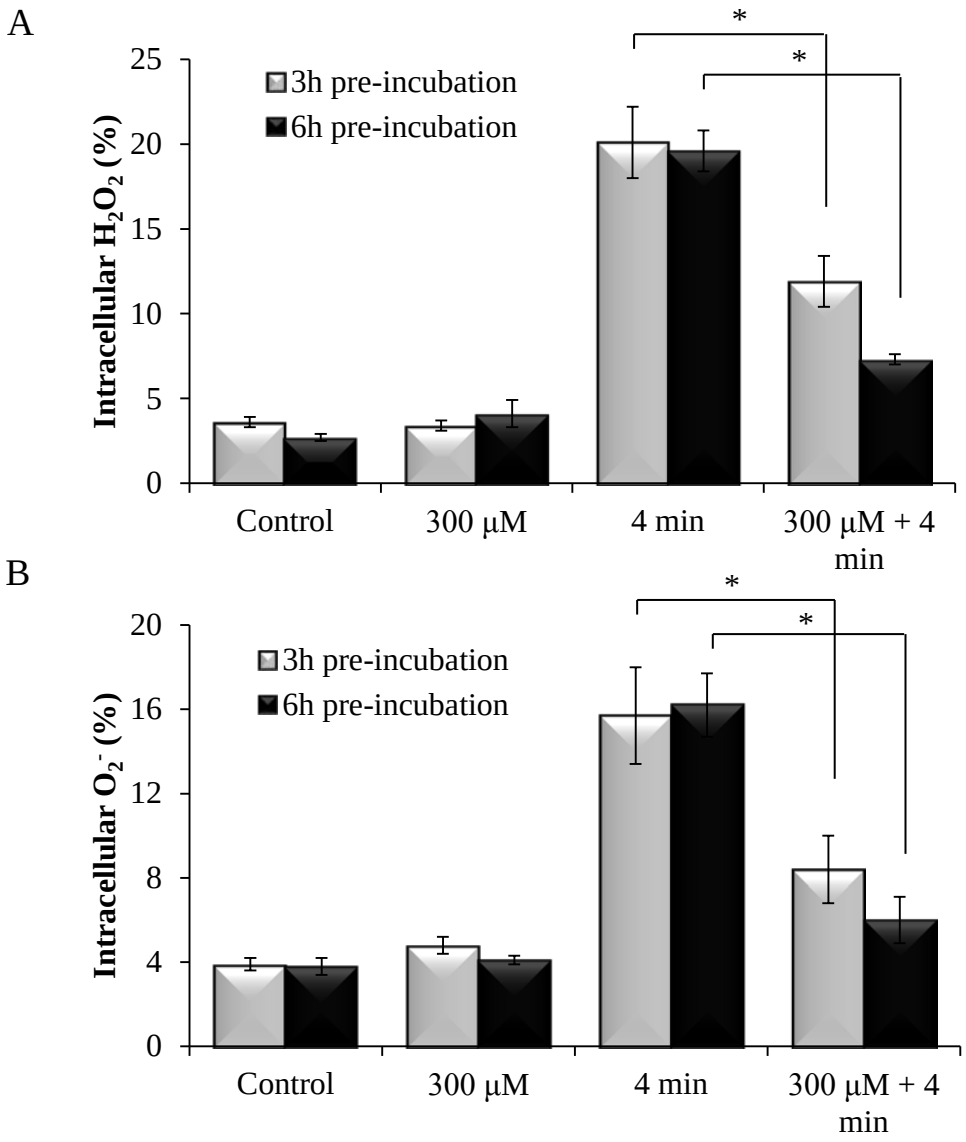

U937 cells were treated with He-CAP for (4 min) in the presence or absence of Pt-NPs. The percentage of cells with elevated level of ROS species were analyzed by flow cytometry immediately after He-CAP. (A) DCFH staining, (B) HE staining. Data are presented as the mean ± SD. *$P \leq 0.05$ as compared with He-CAP treatment alone. Data shown are representative of five independent experiments.

Fig. 12

Effects of Pt-NPs on He-CAP-induced MMP loss in U937 cells, as determined by flow cytometry using TMRM staining

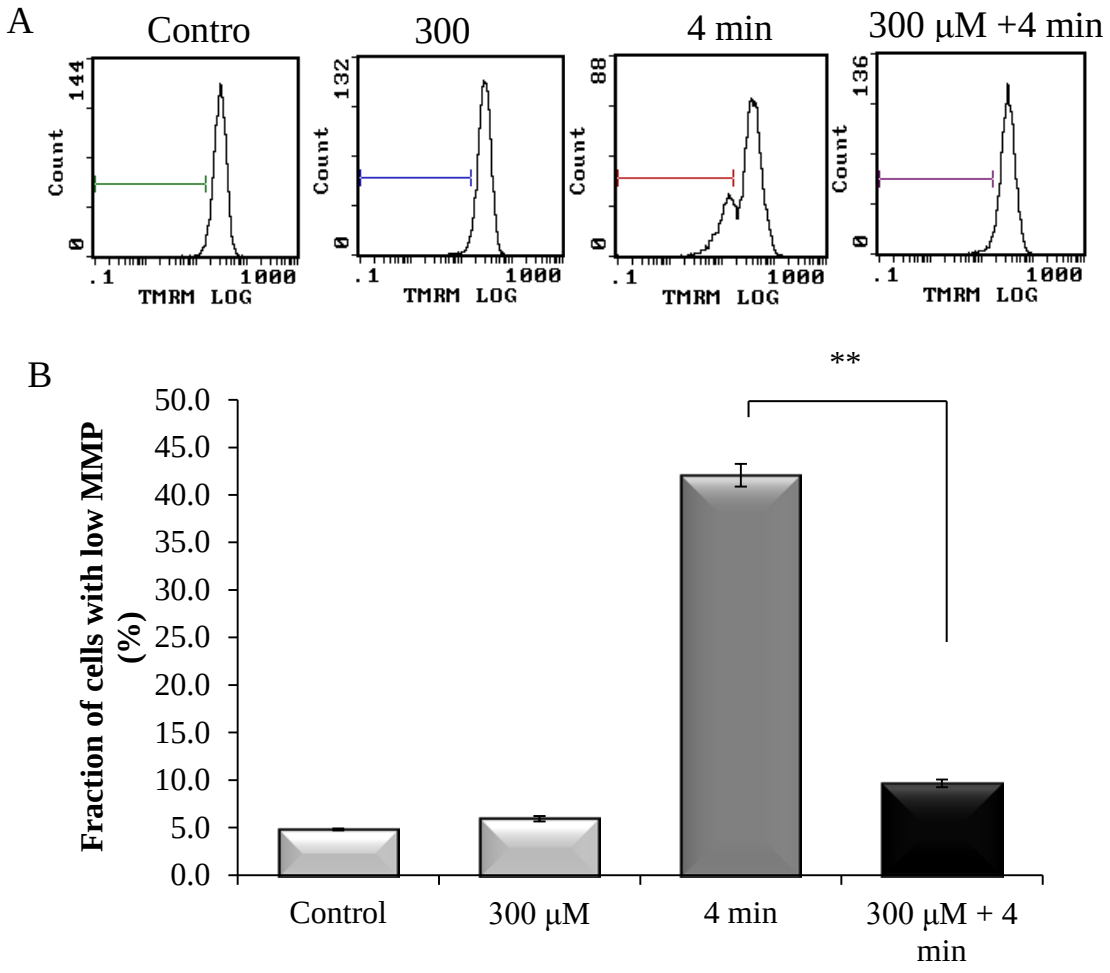

(A) Representative flow cytometric histogram of MMP loss. (B) Increased loss of MMP was observed in the cells treated with the He-CAP alone. Which was decreased in the presence of Pt-NPs. Data are presented as mean ± SD. **P≤0.005 as compared with He-CAP treatment alone. Data shown are representative of five independent experiments.

Fig. 13

Effects of Pt-NPs on He-CAP-induced [Ca^{2+}]i levels.

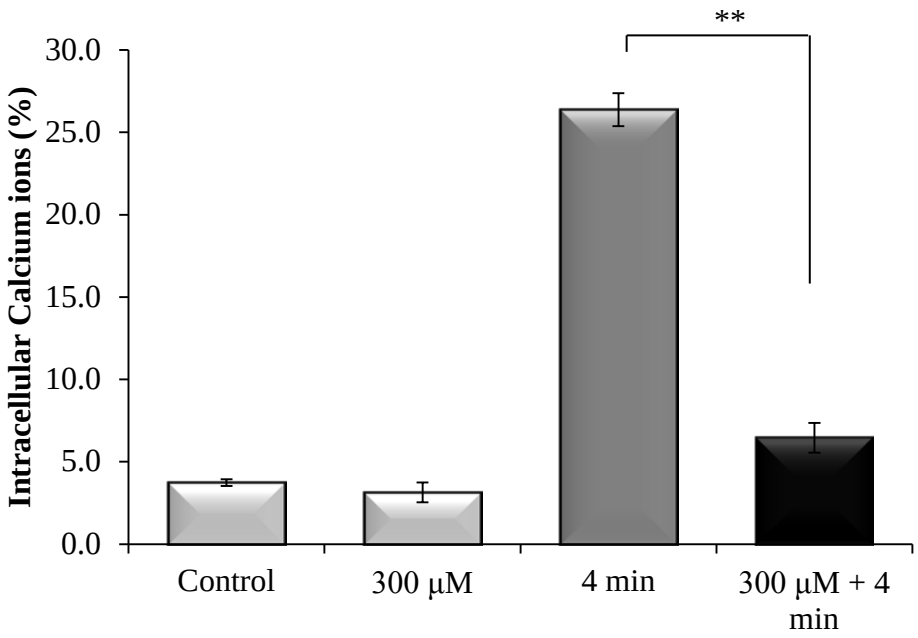

Cells were treated with He-CAP for (4 min) and then harvested 18 h after treatment. Cells were loaded with 5 μM calcium probe Fluo-3/AM for 30 min, and [Ca^{2+}]i level was measured by flow cytometry. Data are presented as mean ± SD. **$P \leq 0.005$, compared with the He-CAP alone. Data shown are representative of five independent experiments.

Fig. 14

Assessment of apoptosis related proteins.

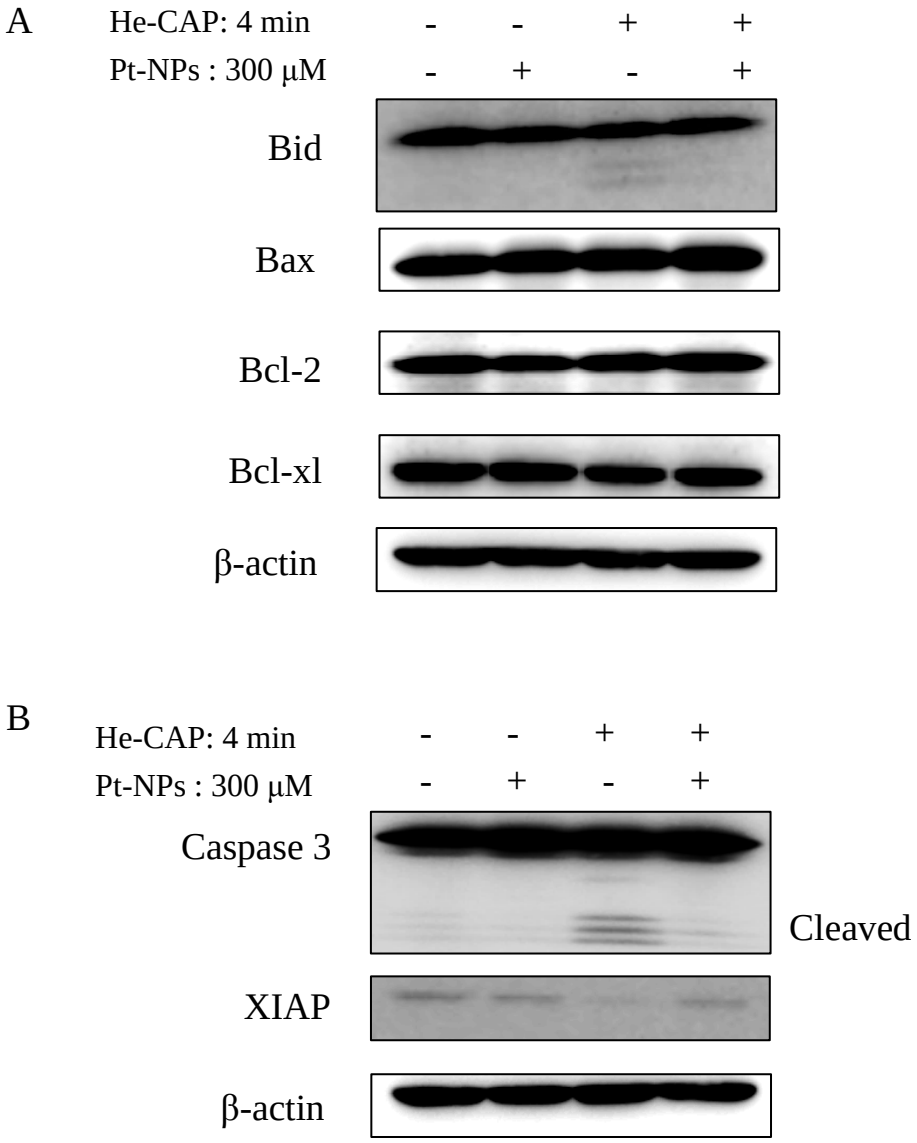

Cells were treated with or without Pt-NPs and, then harvested 18 h after He-CAP treatment. (A) Western blot analysis of Bcl-2 family proteins (B) Changes in the expression levels of caspase-3 and Xiap as detected by western blot analysis.

Fig. 15

Effects of Pt-NPs on He-CAP-induced Fas externalization and caspase-8 activation.

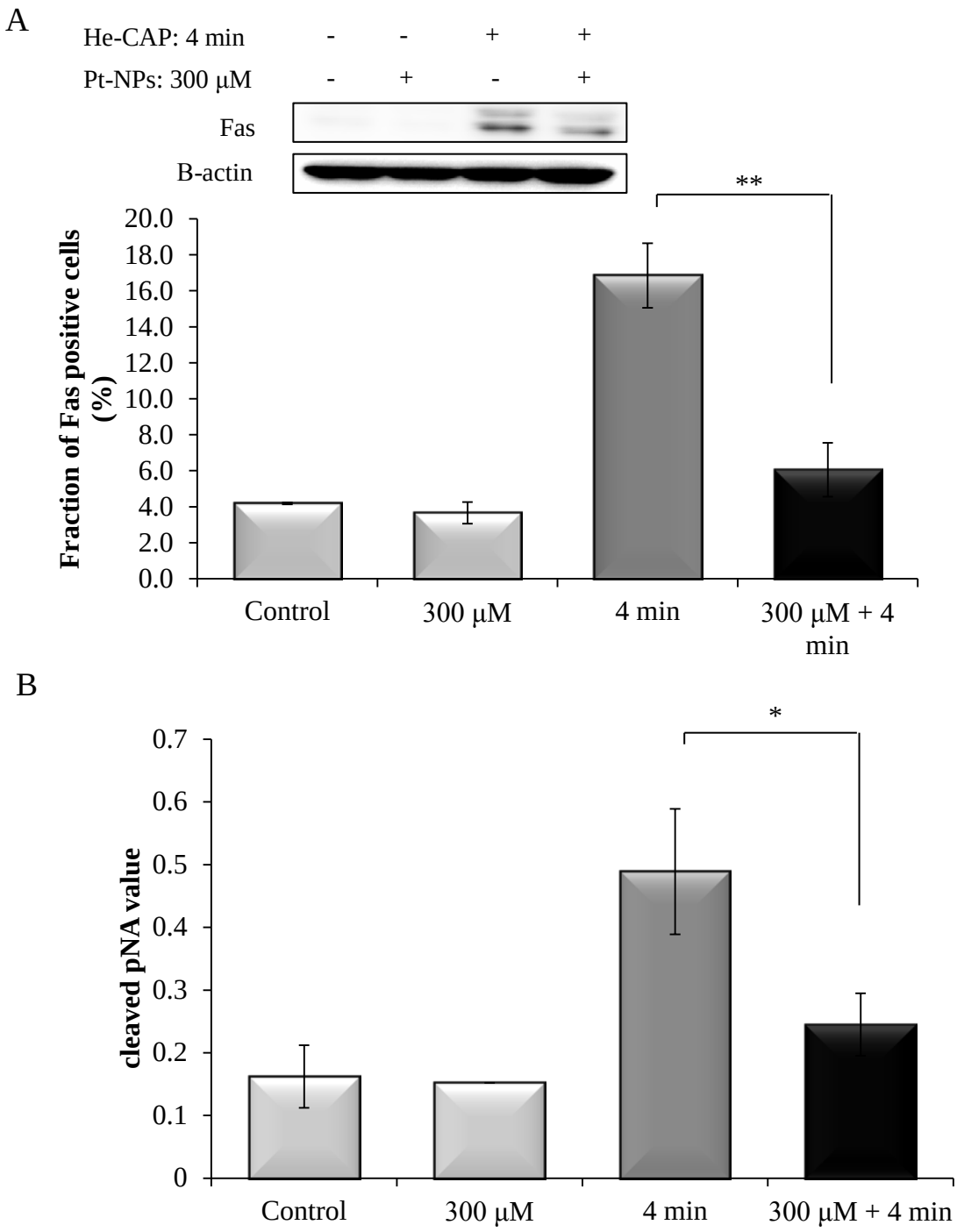

(A) Expression of Fas detected by western blot analysis. Changes in the fraction of U937 cells with Fas externalization were analyzed by flow cytometry using an anti-Fas FITC-conjugated antibody after treatment with He-CAP (4 min) for 18 h in the presence or absence of Pt-NPs. (B) Caspase-8 activity in U937 cells induced by the He-CAP treatment with or without Pt-NPs was also measured with a FLICE/caspase-8 colorimetric protease kit. Data are presented as mean ± SD. *$P \leq 0.05$, **$P \leq 0.005$ compared with the He-CAP alone. Data shown are representative of five independent experiments.

Fig. 16

Effect of Pt-NPs on He-CAP-induced apoptosis in other cell lines.

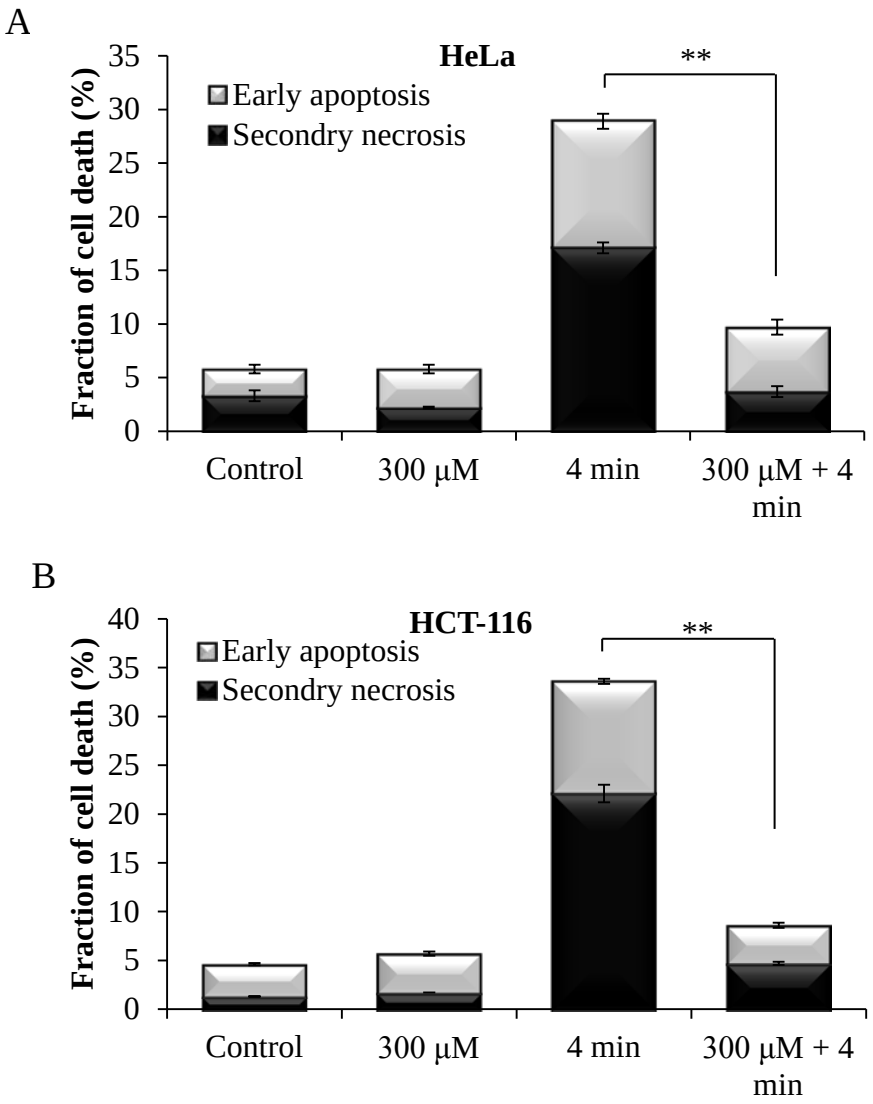

Evaluation of early apoptosis and secondary necrosis by annexin V-FITC/PI staining (A) HeLa cells (B) HCT-116 cells. Data are presented as mean ± SD. **P≤0.005 compared with He-CAP alone. Data shown are representative of five independent experiments.

Fig. 17

Assessment of apoptosis in Molt-4 cells.

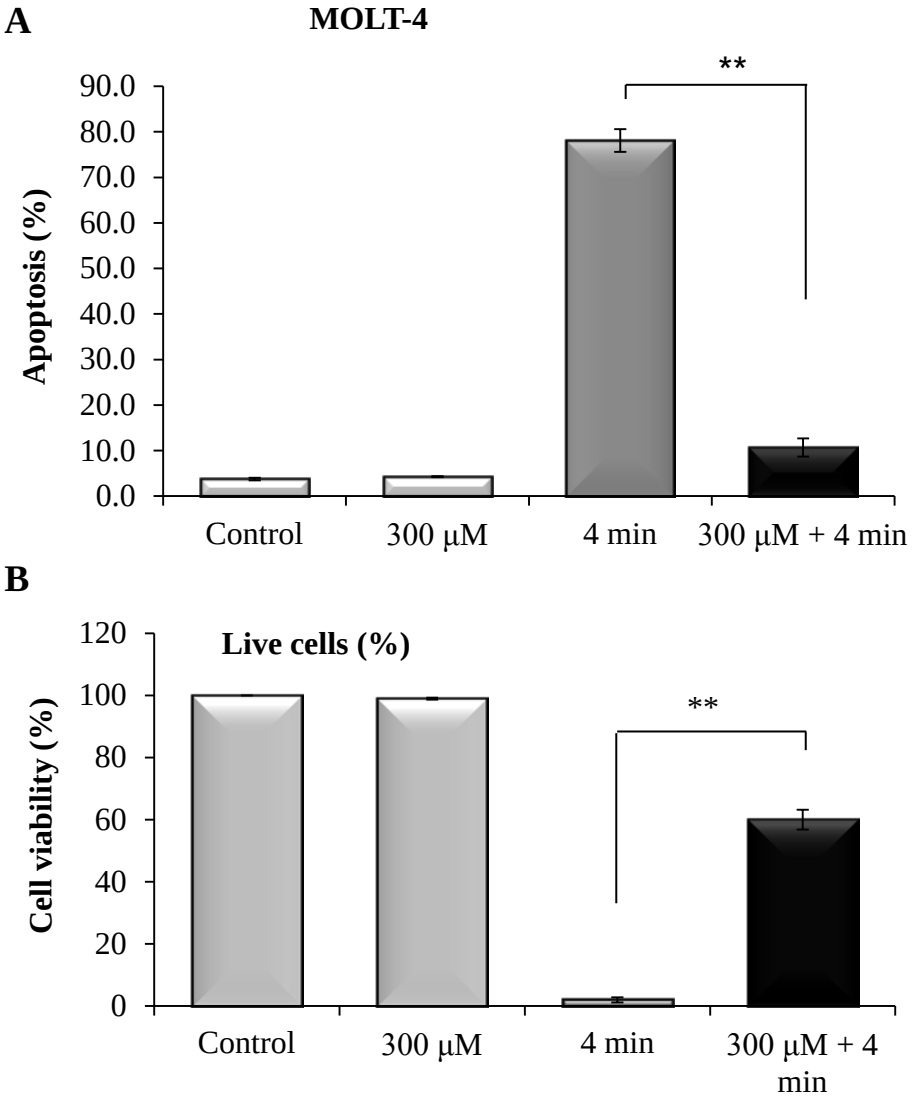

(A) PI staining was carried out 6 h after He-CAP treatment using flow cytometry (B) Viability of cells assessment by using trypan blue exclusion dye. Data are presented as mean ± SD. **P≤0.005. Data shown are representative of five independent experiments.

Fig. 18

Assessment of apoptosis in Jurkat-T cells.

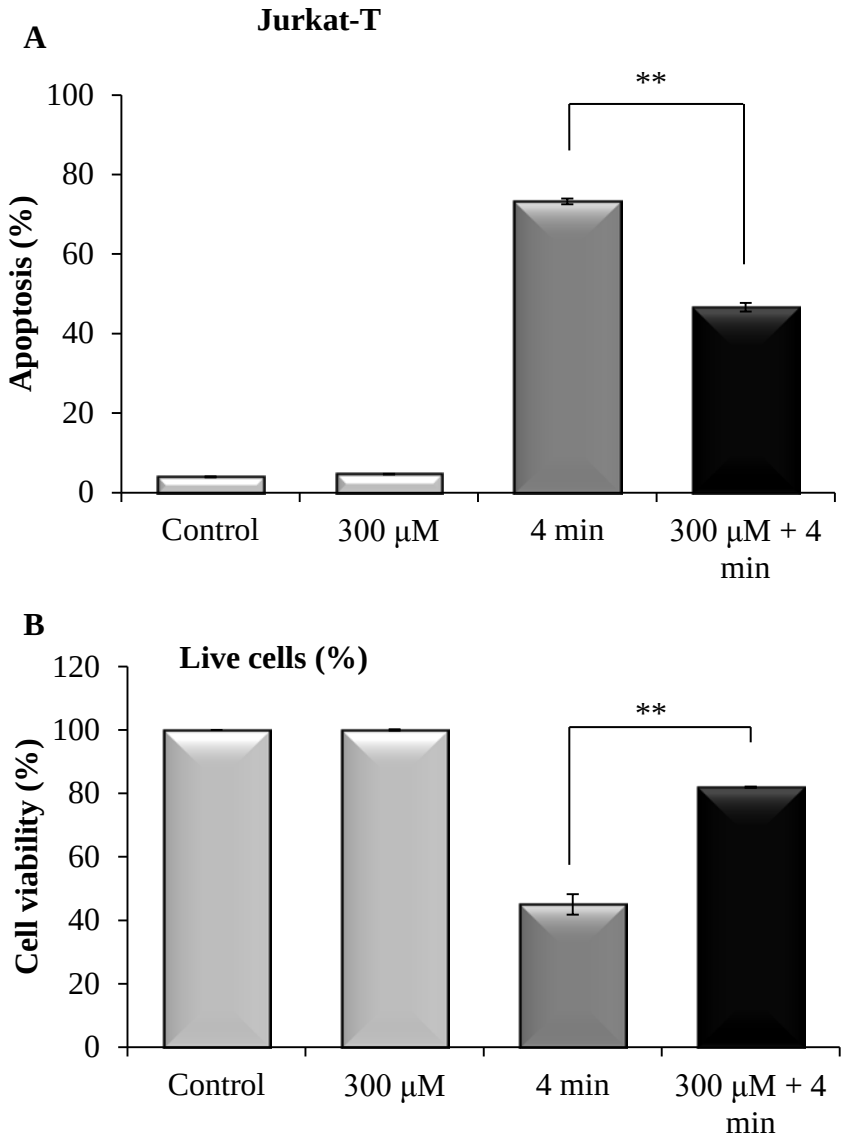

(A) PI staining for flow cytometry and (B) Viability of cells assessment using trypan blue exclusion dye at 6 h after He-CAP treatment in the presence or absence of Pt-NPs at a dose of 300 μM. Data are presented as mean ± SD. **P≤0.005. Data shown are representative of five independent experiments.

Fig. 19

Graphical scheme of the pathways involved in the protective effects of Pt-NPs against He-CAP-induced apoptosis.

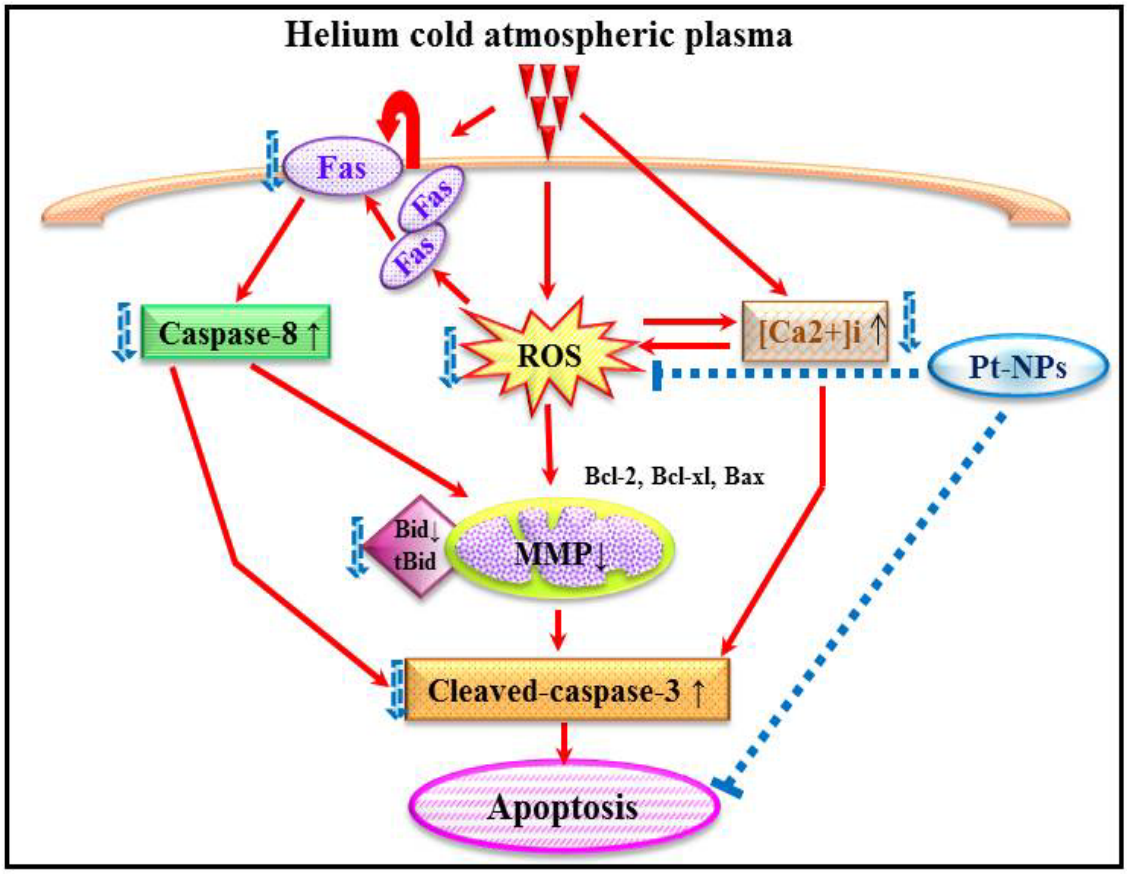

Table. 1

* Indictae statistical significance compared to He-CAP

	Control	Pt-NPs (300 μM)	He-CAP (4 min)	Pt-NPs (300 μM) + He-CAP (4min)
Sub G1	3.7 ± 0.2	3.8 ± 0.8	24 ± 0.4	*9.8 ± 1.2
G0/G1	41.3 ± 0.1	40.7 ± 1.0	30 ± 0.7	38.5 ± 0.6
S phase	33.4 ± 2.6	35 ± 0.6	30 ± 1.5	26.7 ± 0.5
G2/M	18.2 ± 0.7	17.7 ± 0.2	13 ± 1.4	21 ± 1.6

References

1. Kajita M, Hikosaka K, Iitsuka M, Kanayama A, Toshima N, Miyamoto Y. Platinum nanoparticle is a useful scavenger of superoxide anion and hydrogen peroxide. *Free Radic. Res*. 2007; **41**:615–626.
2. Kostova I. Platinum complexes as anticancer agents. *Recent Pat Anti-Cancer Drug Discov*. 2006; **1**:1–22.
3. Yoshihisa Y, Zhao QL, Hassan MA et al. SOD/catalase mimetic platinum nanoparticles inhibit heat-induced apoptosis in human lymphoma U937 and HH cells. *Free Radic. Res*. 2010; **45**:326-335.
4. Asharani PV, Xinyi N, Hande MP, Valiyaveettil S. DNA damage and p-53 mediated growth arrest in human cells treated with platinum nanoparticles. *Nanomedicine*. 2010; **5**:51-64.
5. Toshima N, Yonezawa T. Bimetallic nanoparticles—novel materials for chemical and physical applications. *N. J. Chem*. 1998; **22**:1179–1201.
6. Roucoux A, Schulz J, Patin H. Reduced transition metal colloids: a novel family of reusable catalysts? *Chem Rev*. 2002; **102**:3757–3778.
7. Yoshihisa Y, Honda A, Zhao QL et al. Protective effects of platinum nanoparticles against UV-light-induced epidermal inflammation. *Exp. Dermatol*. 2010; **19**:1000-1006.
8. Onizawa S, Aoshiba K, Kajita M, Miyamoto Y, Nagai A. Platinum nanoparticle antioxidants inhibit pulmonary inflammation in mice exposed to cigarette smoke. *Pulm. Pharmacol. Ther*. 2009; **22**:340-349.
9. Kim J, Takahashi M, Shimizu T et al. Effects of a potent antioxidant, platinum nanoparticle, on the lifespan of Caenorhabditis elegans. *Mech. Ageing. Dev*. 2008; **129**:322-331.

10. Borek C. Antioxidants and Radiation Therapy. *J. Nutr*. 2004; **134**:3207–3209.
11. Riley PA. Free radical in biology: oxidative stress and the effects of ionization radiation. *Int. J. Radiat. Biol*. 1994; **65**:27-33.
12. Miyata H, Doki Y, Yamamoto H et al. Overexpression of CDC25B overrides radiation-induced G2-M arrest and results in increased apoptosis in esophageal cancer cells. *Cancer Res*. 2001; **61**:3188–3193.
13. Corbiere C, Liagre B, Terro F, Beneytout JL. Induction of antiproliferative effect by diosgenin through activation of p53, release of apoptosis-inducing factor (AIF) and modulation of caspase-3 activity in different human cancer cells. *Cell Res*. 2004; **14**:188–196.
14. Sasano N, Enomoto A, Hosoi Y et al. Free radical scavenger Edaravone suppresses X-ray induced apoptosis through p53 inhibition in MOLT-4 cells. *J. Radiat. Res*. 2007; **48**:495-503.
15. Tominaga H, Kodama S, Matsuda N, Suzuki K, Watanabe M. Involvement of reactive oxygen species (ROS) in the induction of genetic instability by radiation. *J. Radiat. Res*. 2004; **45**:181–188
16. Zhang B, Su Y, Ai G, Wang Y, Wang T, Wang F. Involvement of Peroxiredoxin I in protecting cells from radiation-induced death. *J. Radiat. Res*. 2005; **46**:305–312
17. Kong MG, Kroesen G, Morfill G et al. Plasma medicine: an introductory review. *New J. Phys*. 2009; **11**:15012.
18. Kieft IE, Broers JL, Caubet-Hilloutou V, Slaaf DW, Ramaekers FC, Stoffels E. Electric discharge plasmas influence attachment of cultured CHO K1 cells. *Bioelectromagnetics*. 2004; **25**:362-368.
19. Hoffmann C, Berganza C, Zhang J. Cold Atmospheric Plasma: methods of

production and application in dentistry and oncology. *Med. Gas Res.* 2013; **3**:21.

20. Stoffels E, Flikweert AJ, Stoffels WW, Kroesen GMW. Plasma needle: a non-destructive atmospheric plasma source for fine surface treatment of (bio)materials. *Plasma Sources Sci. Technol*. 2002; **11**:383-388.
21. Kim SJ, Chung TH, Bae SH, Leem SH. Induction of apoptosis in human breast cancer cells by a pulsed atmospheric pressure plasma jet. *Appl. Phys. Lett*. 2010; **97**:023702-3.
22. Kalghatgi SU, Fridman G, Cooper M et al. Mechanism of blood coagulation by nonthermal atmospheric pressure dielectric barrier discharge plasma. *IEEE Trans. Plasma Sci*. 2007; **35**:1559-1566.
23. Arndt S, Unger P, Wacker E et al. Cold Atmospheric Plasma (CAP) changes gene expression of key molecules of the wound healing machinery and improves wound healing in vitro and in vivo. *PLos one*. 2013; **8**:e79325.
24. Fridman G, Friedman G, Gutsol A, Shekhter AB, Vasilets VN, Fridman A. Applied Plasma Medicine. *Plasma Process Polym*. 2008; **5**:503-533.
25. Soloshenko IA, Tsiolko VV, Khomich VA et al. Sterilization of medical products in low-pressure glow discharges. *Plasma. Phys. Rep*. 2000; **26**:792–800.
26. Sladek REJ, Stoffels E, Walraven R, Tielbeek PJA, Koolhoven RA. Plasma treatment of dental cavities: a feasibility study. *IEEE Trans. Plasma Sci.* 2004; **32:** 1540–1543.
27. Vandamme M, Robert E, Dozias S et al. Response of human glioma U87 xenografted on mice to non thermal plasma treatment. *Plasma Med*. 2011; **1**:27-43.
28. Vandamme M, Robert E, Lerondel S et al. ROS implication in a new antitumor strategy based on non-thermal plasma. *Int. J. Cancer*. 2012; **130**:2185-2194.

29. Lupu AR, Georgescu N. Cold atmospheric plasma jet effects on V79-4 cells. *Roum*. *Arch*. *Microbiol*. *Immunol*. 2010; **69**: 67-74.

30. Arndt S, Wacker E, Li YF et al. Cold atmospheric plasma, a new strategy to induce senescence in melanoma cells. *Exp*. *Dermatol*. 2013; **22**:284-289.

31. Sellins KS, Cohen JJ. Gene induction by gamma-irradiation leads to DNA fragmentation in lymphocytes. *J. Immunol*. 1987; **139**:3199–3206.

32. Royall JA, Ischiropoulos H. Evaluation of 2`,7`-dichlorofluorescin and dihydrorhodamine 123 as fluorescent probes for intracellular H_2O_2 in cultured endothelial cells. *Arch. Biochem. Biophys*. 1993; **302**:348–355.

33. Setsukinai KI, Urano Y, Kakinumas K, Majima HJ, Nagano T. Development of novel Fuorescence probes that can reliably detect Reactive oxygen species and distinguish specific species. *J. Biol. Chem*. 2003; **278**:3170-3175.

34. Bhattacharya R, Mukherjee P. Biological properties of ‘‘naked’’ metal nanoparticles. *Adv. Drug. Deliv. Rev*. 2008; **60**:1289–1306.

35. Jamieson ER, Lippard SJ. Structure, recognition, and processing of cisplatin–DNA adducts. *Chem. Rev*. 1999; **99**:2467–2498.

36. Rehman MU, Yoshihisa Y, Miyamoto Y, Shimizu T. The anti-inflammatory effect of platinum nanoparticles on the lipopolysaccharide induced inflammatory response in RAW 264.7 macrophages. *Inflamm. Res*. 2012; **61**:1177-1185.

37. Zhang X, Zhou X, Chen R, Zhang H. Radiosensitization by inhibiting complex I activity in human hepatoma HepG2 cells to X-ray radiation. *J. Radiat. Res*. 2012; **53**:257-263.

38. Hall EJ. The physics and chemistry of radiation absorption. In: Hall EJ (ed) Radiobiology for the Radiologist, 7th edn. New York, Lippincott for Williams and

Wilkins, 2010; p 1-16.

39. Cui ZG, Kondo T, Feril JLB, Waki K, Inanami O, Kuwabara M. Effects of antioxidants on x-ray or hyperthermia induced apoptosis in human lymphoma U937 cells. *Apoptosis*. 2004; **9**:757-763.
40. Salganik RI. The benefits and hazards of antioxidants: controlling apoptosis and other protective mechanism in cancer patients and the human population. *J. Am. Coll. Nutr*. 2001; **20**:464S-475S.
41. Bhuyan BK, Goppi VE. Cell cycle specific inhibitors. *Pharmac. Therap*. 1989; **42**:307-348.
42. Yamada T, Ohyama H. Radiation-induced interphase death of rat thymocytes in internally programmed (apoptosis). *Int. J. Radiat. Biol*. 1988; **53**:65-75.
43. Cui ZG, Kondo T, Ogawa R et al. Enhancement of radiation-induced apoptosis by 6-formylpterin. *Free Radic. Res*. 2004; **38**:363–373.
44. Yu DY, Zhao QL, Wei ZL et al. Enhancement of radiation induced apoptosis of human lymphoma U937 cells by sanazole. *Apoptosis*. 2009; **14**:655-664.
45. Nitobe J, Yamaguchi S, Okuyama M et al. Reactive oxygen species regulate FLICE inhibitory protein (FLIP) and susceptibility to Fas-mediated apoptosis in cardiac myocytes. *Cardiovasc. Res*. 2003; **57**:119–128.
46. Embree-Ku M, Venturini D, Boekelheide K. Fas is involved in the p53-dependent apoptotic response to ionizing radiation in mouse testis. *Biol. Reprod*. 2002; **66**:1456–1461.
47. Strasser A, Newton K. FADD/MORT1, a signal transducer that can promote cell death or cell growth. *Int. J. Biochem. Cell Biol*. 1999; **31**:533–537.
48. Yin XM. Signal transduction mediated by Bid, a pro-death Bcl-2 family proteins,

connects the death receptor and mitochondria apoptosis pathways. *Cell Res*. 2000; **10**:161–167.

49. Wang X. The expanding role of mitochondria in apoptosis. *Genes. Dev*. 2001; **15**:2922-2933.
50. Campion SN, Sandrof MA, Yamasaki H, Boekelheide K. Suppression of radiation-induced testicular germ cell apoptosis by 2,5-hexanedione pretreatment. III. Candidate gene analysis identifies a role for Fas in the attenuation of X-ray–induced apoptosis. *Toxicol. Sci*. 2010; **117**:466-474.
51. Kolesnick R, Fuks Z. Radiation and ceramide-induced apoptosis. *Oncogene*. 2003; **22**:5897-5906.
52. Nomura M, Yoshimura Y, Kikuiri T et al. Platinum nano particles suppress Osteoclastogenesis through scavenging of reactive oxygen species produced in RAW 264.7 cells. *J. Pharmacol. Sci*. 2011; **117**:243-252.
53. Onizawa S, Aoshiba K, Kajita M, Miyamoto Y, Nagai A. Platinum nanoparticle antioxidants inhibit pulmonary inflammation in mice exposed to cigarette smoke. *Pulm. Pharmscol. Ther*. 2009; **22**:340-349.
54. Chen M, Wang J. Initiator caspases in apoptosis signaling pathways. *Apoptosis*. 2002; **7**:313-319.
55. Granville DJ,Gottlieb RA. Mitochondria: regulators of cell death and survival. *Scientific World Journal*. 2002; **2**:1569-1578.
56. Esposti MD. The roles of Bid. *Apoptosis*. 2002; **7**:433-440.
57. Li H, Zhu H, Xu CJ, Yuan J. Cleavage of Bid by caspase8 mediates the mitochondrial damage in the Fas pathway of apoptosis. *Cell*. 1998; **94**:491-501.
58. Burda C, Chen X, Narayanan R, El-Sayed MA. Chemistry and properties of

nanocrystals of different shapes. *Chem. Rev*. 2005; **105**:1025–1102.

59. Mulvaney P. Surface plasma on spectroscopy of nanosized metal particles. *Langmuir*. 1996; **1**:788–798.
60. Gehrke H, Pelka J, Hartinger CG et al. Platinum nanoparticles and their cellular uptake and DNA platination at non-cytotoxic concentrations. *Arch. Toxicol*. 2011; **85**:799-812.
61. Yoshida H, Ishikawa Y, Yamagiwa T et al. Administration of nano-sized platinum colloid reduces the volume of cerebral ischemia by inhibition of increased reactive oxygen species in a rat middle cerebral artery occlusion stroke model (abstract). *Society for Neuroscience*. 2003.
62. Kalghatgi S, Kelly CM, Cerchar E et al. Effects of non-thermal plasma on mammalian cells. *PLoS One*. 2011; **6**. e16270.
63. Yan X, Xiong Z, Zou F et al. Plasma-induced death of HepG2 cancer cells: intracellular effects of reactive species. *Plasma. Processes. Polymers*. 2012; **9**:59–66.
64. Iseki S, Nakamura K, Hayashi M et al. Selective killing of ovarian cancer cells through induction of apoptosis by nonequilibrium atmospheric pressure plasma. *Appl. Phys. Lett*. 2012; **100**:113702.
65. Thiyagarajan M, Waldbeser L, Whitmill A. THP-1 leukemia cancer treatment using a portable plasma device. *Stud. Health. Technol. Inform*. 2012; **173**:515–517.
66. Bienert GP, Moller ALB, Kristiansen KA et al. Specific aquaporins facilitate the diffusion of hydrogen peroxide across membranes. *J. Biol. Chem*. 2007; **282**:1183–1192.
67. Bienert GP, Schjoerring JK, Jahn TP. Membrane transport of hydrogen peroxide.

Biochim. *Biophys*. *Acta*. 2006; **1758**: 994–1003.

68. Kalghatgi S, Friedman G, Fridman A, Clyne AM. Endothelial cell proliferation is enhanced by low dose non-thermal plasma through fibroblast growth factor-2 release. *Ann*. *Biomed*. *Eng*. 2010; **38**:748–757.
69. Slater TF. Free-radical mechanisms in tissue injury. *J. Biochem*. 1984; **222**:1–15.
70. Finkel T. Signal transduction by reactive oxygen species in non-phagocytic cells. J. *Leukoc. Biol*. 1999; **65**:337–340.
71. Xu D, Liu D, Wang B et al. In situ OH generation from O_2^- and H_2O_2 plays a critical role in Plasma induced cell death. *PLos One*. 2015; **10**:e0128205.
72. Tsujimoto Y, Shimizu S. Role of the mitochondrial membrane permeability transition in cell death. *Apoptosis*. 2007; **12**: 835–840.
73. Ahn HJ, Kim KI, Kim G, Moon E, Yang SS, Lee JS. Atmospheric-pressure plasma jet induces apoptosis involving mitochondria via generation of free radicals. *PLoS On*e. 2011; **6**:e28154.

Publication list

Published papers:

1. **Jawaid P**, Rehman MU, Yoshihisa Y, Li P, Zhao QL, Hassan MA, Miyamoto Y, Shimizu T, Kondo T. Effects of SOD/catalase mimetic platinum nanoparticles on radiation-induced apoptosis in human lymphoma U937 cells. Apoptosis. 2014 Jun;19(6):1006-16. doi: 10.1007/s10495-014-0972-5 (Impact Factor: 3.6)

2. **Jawaid P**, Rehman MU, Zhao QL, Miyamoto Y, Takeda K, Ishikawa K, Hori M, Shimizu T, Kondo T. Platinum nanoparticles prevent from Helium based cold atmospheric plasma-induced apoptosis via suppression of ROS generation. Journal of Cellular and Molecular Medicine. (Accepted with major revision) (Impact Factor: 4.1)

Acknowledgement

There are many people's I would like to acknowledge who have made this thesis possible. Firstly, I would like to extend my sincere gratitude to my supervisor **Professor Takashi Kondo** Department of Radiological Sciences, Graduate school of medicine and Pharmaceutical Sciences University of Toyama, for his enormous support, supervision, encouragement, stimulating confidence and guidance during the four years of my PhD course. He not only taught me the technical knowledge on my research, but also taught me how to communicate with other persons, and how to show myself better. I thanked to Prof. Takashi Kondo to provide me the opportunity to pursue my dream of research and education in his laboratory. He is the role model for me. I am grateful to **Associate Prof. Ryohei Ogawa** and **Assistant Prof. Qing-Li Zhao** for his guidance throughout my period of research. I would like to thanks to all my colleagues and friends in Japan for sharing their minds, skills and happiness with me.

My endless thanks and heartiest gratitude goes to Prof. Dr. Khan Usman ghani, for his support in my research carrier and also in my life. I would like to express my sincere thanks to Madam Sadia Rashid, President, Hamdard Foundation, Pakistan and Prof. Dr. Hk. Abdul Hannan, Vice Chancelor, Hamdard University, Pakistan and to all my teachers, colleagues, staff of Faculty for their love and support.

Finally, I want my heartfelt thanks to my family my **mother** and **father** who worked hard to get me to continue my education till now and always support my thought, giving me love, care, encouragement and support wherever, whenever. Special thanks to my husband **Mati Ur Rehman**, for his uncounted love, special care, advice, encouragement and deep support during all the time of my study in Japan. I would not finish my PhD course without their strong support.

Lastly I would like thank to this beautiful country Japan, which has thought me the new chapter of my life.

Thank you all!!! Thank you Japan!!!

Paras Jawaid

University of Toyama

March 2016